



HAL
open science

Variable origin of clinopyroxene megacrysts carried by Cenozoic volcanic rocks from the eastern limb of Central European Volcanic Province (SE Germany and SW Poland)

Magdalena Matusiak-Malek, Jacek Puziewicz, Theodoros Ntaflou, Alan Woodland, Laura Uenver-Thiele, Jörg Büchner, Michel Grégoire, Sonja Aulbach

► To cite this version:

Magdalena Matusiak-Malek, Jacek Puziewicz, Theodoros Ntaflou, Alan Woodland, Laura Uenver-Thiele, et al.. Variable origin of clinopyroxene megacrysts carried by Cenozoic volcanic rocks from the eastern limb of Central European Volcanic Province (SE Germany and SW Poland). *Lithos*, 2021, 382, 10.1016/j.lithos.2020.105936 . insu-03661476

HAL Id: insu-03661476

<https://insu.hal.science/insu-03661476>

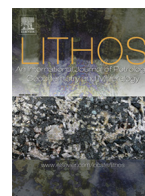
Submitted on 7 May 2022

HAL is a multi-disciplinary open access archive for the deposit and dissemination of scientific research documents, whether they are published or not. The documents may come from teaching and research institutions in France or abroad, or from public or private research centers.

L'archive ouverte pluridisciplinaire **HAL**, est destinée au dépôt et à la diffusion de documents scientifiques de niveau recherche, publiés ou non, émanant des établissements d'enseignement et de recherche français ou étrangers, des laboratoires publics ou privés.



Distributed under a Creative Commons Attribution 4.0 International License



Research Article

Variable origin of clinopyroxene megacrysts carried by Cenozoic volcanic rocks from the eastern limb of Central European Volcanic Province (SE Germany and SW Poland)



Magdalena Matusiak-Małek^{a,*}, Jacek Puziewicz^a, Theodoros Ntaflos^b, Alan Woodland^c, Laura Uenver-Thiele^c, Jörg Büchner^d, Michel Grégoire^e, Sonja Aulbach^{c,f}

^a University of Wrocław, Institute of Geological Sciences, pl. M. Borna 9, 50-204 Wrocław, Poland

^b University of Vienna, Department of Lithospheric Research, Althanstrasse 4, 1090 Wien, Austria

^c Goethe-University, Frankfurt, Institute of Geoscience, Altenhoferallee 1, 60438 Frankfurt, Germany

^d Senckenberg Museum für Naturkunde Görlitz, PF300154, 02806 Görlitz, Saxony, Germany

^e Géosciences Environnement Toulouse, CNRS-CNES-IRD Université Toulouse III, OMP, 14 Av. Eduard Belin, 31400 Toulouse, France

^f Frankfurt Isotope and Element Research Center (FIERCE), Goethe-University Frankfurt, Frankfurt am Main, Germany

ARTICLE INFO

Article history:

Received 18 February 2020

Received in revised form 13 September 2020

Accepted 12 December 2020

Available online 20 December 2020

ABSTRACT

Clinopyroxene megacrysts occurring in Cenozoic mafic alkaline volcanic rocks from the northern margin of the Bohemian Massif (SW Poland, SE Germany) could be subdivided by colour and Mg# ($\text{Mg}/(\text{Mg} + \text{Fe}^{\text{tot}})$) in three groups. Megacryst with the highest Mg# = 90.0–91.5 (“high Mg#”, HMg#) is transparent and strongly Light Rare Earth Element (LREE) depleted and contains abundant orthopyroxene lamellae. The clinopyroxene megacrysts with “medium Mg#” (MMg#) values (76.8–83.4) are transparent to light grey and are all LREE-enriched. The group with the lowest Mg# (LMg#; 62.2–74.6) is intensively coloured (from grey to green) and may enclose apatite, Ti-magnetite or pseudomorphs after amphibole. The “low Mg#” (LMg#) clinopyroxenes are LREE-enriched, and some display positive Zr–Hf anomalies.

The single HMg# megacryst records pressures ~1 GPa and temperature of 1280 °C, pointing to its mantle origin. It is the first megacryst described in European lavas and possibly worldwide, which shows affinity to Depleted MORB Mantle (DMM). The MMg# megacrysts formed from fractionating mafic magmas at variable pressures and temperatures – from those corresponding to mantle depths (>1 GPa, 1230–1350 °C) to lower/middle crustal values (0.5–0.9 GPa, 1120–1150 °C). The parental melts for this group are isotopically related to the Cenozoic volcanic rocks from the study area. The LMg# megacrysts crystallized from strongly alkaline melts, mostly at lower- to middle-crustal pressures (0.4–1.0 GPa). Their parental melts were also related to Cenozoic volcanism, but their strongly evolved nature resulted in local, but significant enrichment in Zr and Hf. The LMg# megacrysts from three localities in Poland are the first evidence of strongly alkaline magmatism in the north-easternmost part of Cenozoic European Volcanic Province.

© 2020 The Author(s). Published by Elsevier B.V. This is an open access article under the CC BY license (<http://creativecommons.org/licenses/by/4.0/>).

1. Introduction

Megacrysts are a common constituent of ultramafic to mafic alkaline volcanic rocks. In their original meaning (Dawson, 1980), megacrysts were considered as monocrystals of uncertain origin, whose size exceeds 1 cm. Lately, this definition has been eased, due to possible mechanical destruction during ascent (or even during mining) resulting in smaller size-crystals (Kargin et al., 2017; Pivin et al., 2009). Megacrysts may occur in alkaline basalts as well as in kimberlites

and may be formed by numerous species of minerals: pyroxene, garnet, olivine, spinel, ilmenite, amphibole, biotite, apatite, plagioclase, alkali feldspar, corundum, zircons, etc. (Gernon et al., 2016; Righter and Carmichael, 1993; Shaw and Eyzaguirre, 2000; Upton et al., 2009) among which clinopyroxene is far the most common one (e.g. Akinin et al., 2005; Dobosi and Jenner, 1999; Liu and Ying, 2019; Shaw and Eyzaguirre, 2000; Woodland and Jugo, 2007). Origin of clinopyroxene megacrysts is debatable, but three major mechanisms of their formation are suggested in the literature:

- 1) Formation as high pressure precipitates from the melt that carried it to the surface (host melt); in this case the megacrysts are phenocrysts (Streck, 2008) in chemical equilibrium with the host melt

* Corresponding author.

E-mail address: magdalena.matusiak-malek@uwr.edu.pl (M. Matusiak-Małek).

- and inherit its isotopic composition (e.g. Akinin et al., 2005; Dobosi and Jenner, 1999; Shaw and Eyzaguirre, 2000);
- 2) Formation as high pressure precipitates from melts having genetic affinities to the host one; this kind of megacrysts (antecrysts) often serves as a probe of melts which have never reached the surface (e.g. Kopylova et al., 2009; Liu and Ying, 2019; Rankenburg et al., 2004; Roberts et al., 2019);
 - 3) Formation due to disintegration of peridotitic or pyroxenitic xenoliths (Akinin et al., 2005; He et al., 2013; Dobosi et al., 2003; Righter and Carmichael, 1993), production of Cr-rich megacrystic clinopyroxene was suggested also due to reaction of melt with mantle peridotite (Liu and Ying, 2019; Bussweiler et al., 2018; Kargin et al., 2017; He et al., 2013); megacrysts of this type (xenocrysts) are in disequilibrium with its host melt and may show significant differences in isotopic composition.

Megacrysts of variable origin may occur in single locality/area pointing to the complicated structure of lithosphere or multi-stage evolution of magmatic systems (e.g. Ashchepkov, 2011; Liu and Ying, 2019; Schmidt et al., 2016; Upton et al., 1999; Woodland and Jugo, 2007).

Interpretation of a megacryst's compositions is often challenging, as by definition they are monomineralic and some information (e.g. equilibrium phase assemblages, oxygen fugacity) cannot be deciphered. Some of them, however, enclose mineral inclusions (e.g. opaque minerals, apatite, olivine and others), which allow assessment of the conditions of origin (O'Reilly and Griffin, 2000; Patiño Douce et al., 2011).

In this study we discuss possible origins and conditions of formation of clinopyroxene megacryst suite from mafic alkaline volcanic rocks from SW Poland and SE Germany (Fig. 1), which comprises the eastern part of the Cenozoic Central European Volcanic Province (CEVP; Wimmenauer, 1974). Clinopyroxene megacrysts from this area were mentioned (but not discussed in detail) in a few studies dedicated to petrology of mantle xenoliths (e.g. Kozłowska Koch, 1981; Puziewicz et al., 2011), but only the study by Lipa et al. (2014) was entirely devoted to megacrysts. Puziewicz et al. (2011) interpreted clinopyroxene megacrysts from Księginki as high-pressure (1.0–1.5 GPa) precipitates from a mafic melt, while Lipa et al. (2014) suggested that clinopyroxene megacrysts from Ostrzyca Proboszczowicka crystallized from a fractionated alkaline mafic magma at crustal depths. In this study, we argue that megacryst suite from this region is mostly of magmatic origin and records the polybaric fractionation of variable mafic to intermediate silicate magmas related to Cenozoic volcanism; the evolution paths of the melts had numerous local variations depending from composition of the parental melt as well as P-T conditions. Based on the composition of the megacrysts we give first evidence for strongly alkaline magmatism in Polish part of Central European Volcanic Province. One of the forty-two studied megacrysts samples appears to have originated from a depleted MORB mantle domain (DMM) and is the first of this kind to be described.

2. Geological setting

Cenozoic lavas occurring in SE Germany and SW Poland (Lusatia and Lower Silesia regions; Lusatia refers to historic region mostly in E Germany, located west from Lubań, Lower Silesia is an administrative region in SW Poland; Fig. 1) represent some of the numerous volcanic centres widespread in western and central Europe and termed as Central European Volcanic Province (CEVP; Wimmenauer, 1974; Wilson and Downes, 2006). It originated due to large-scale rifting of the foreland of the Alpine orogen since the late Cretaceous, which affected the Variscan basement in France, Germany, Czechia and Poland (Dèzes et al., 2004). Most volcanic rocks occurring in the eastern part of CEVP are concentrated in the Eger (Ohře) Rift (Bohemian Massif) in Czechia (Ulrych et al., 2011). The northernmost part of the CEVP is located in SW Poland and SE Germany and includes the NE prolongation of the

rift and minor volcanic rocks related to the Labe-Odra fault system, perpendicular to the rift axis (Fig. 1). In the area of Lower Silesia more than 300 occurrences (Badura et al., 2006) of basic rocks (mostly basanites and nephelinites; Ntaflos and Puziewicz, 2013; Ladenberger et al., 2004) were identified, while in Lusatia over 1000 volcanic structures formed mostly of nephelinites, basanites and tephrites are known (Büchner et al., 2015). The mafic melts were formed due to low degree melting of asthenospheric mantle, possibly contaminated with low amounts of CO₂ (Ntaflos and Puziewicz, 2013). The isotopic ratios of the volcanic rocks range between HIMU and EMI sources, thus minor contamination with crustal material is possible (Ladenberger et al., 2004).

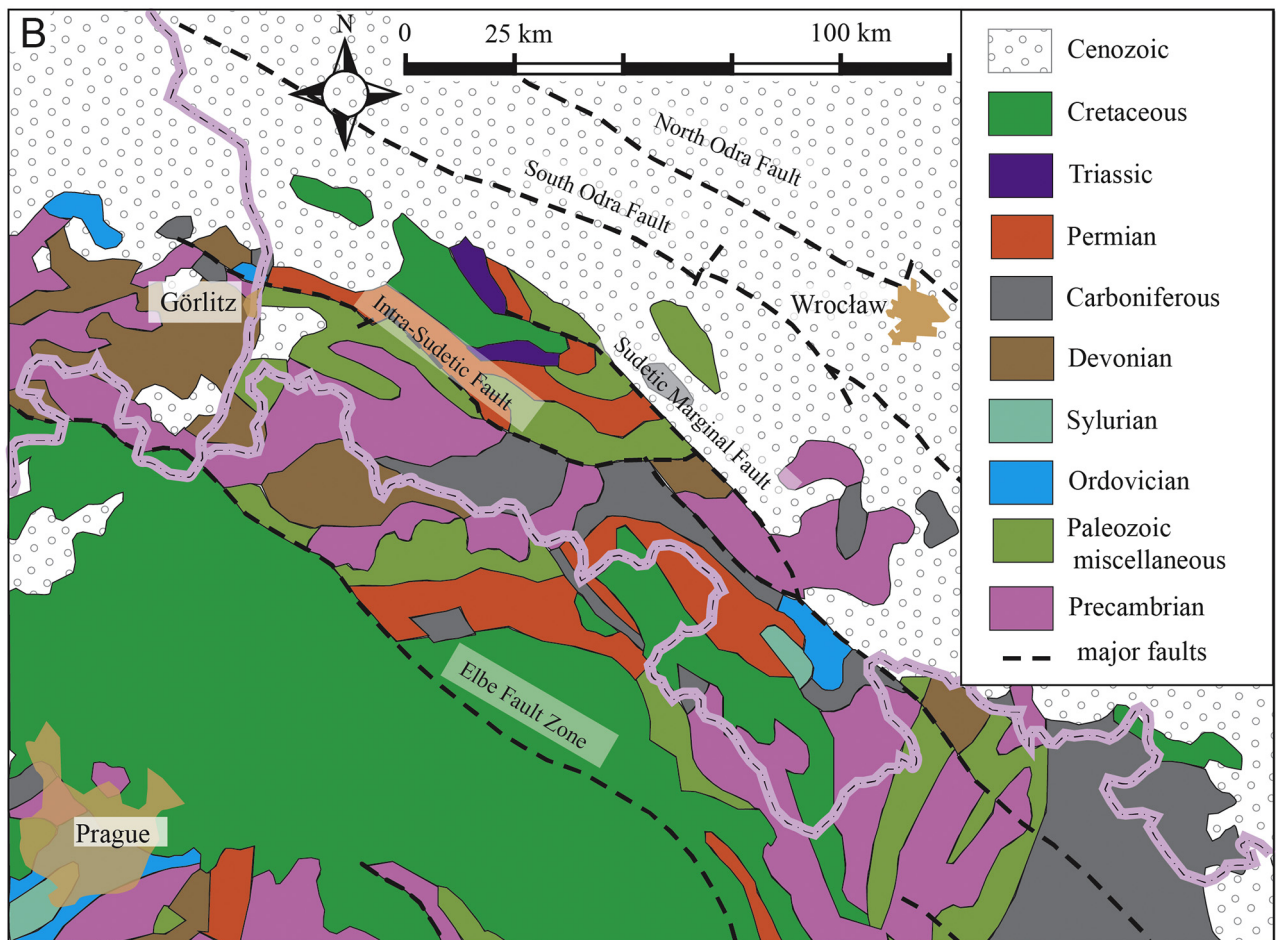
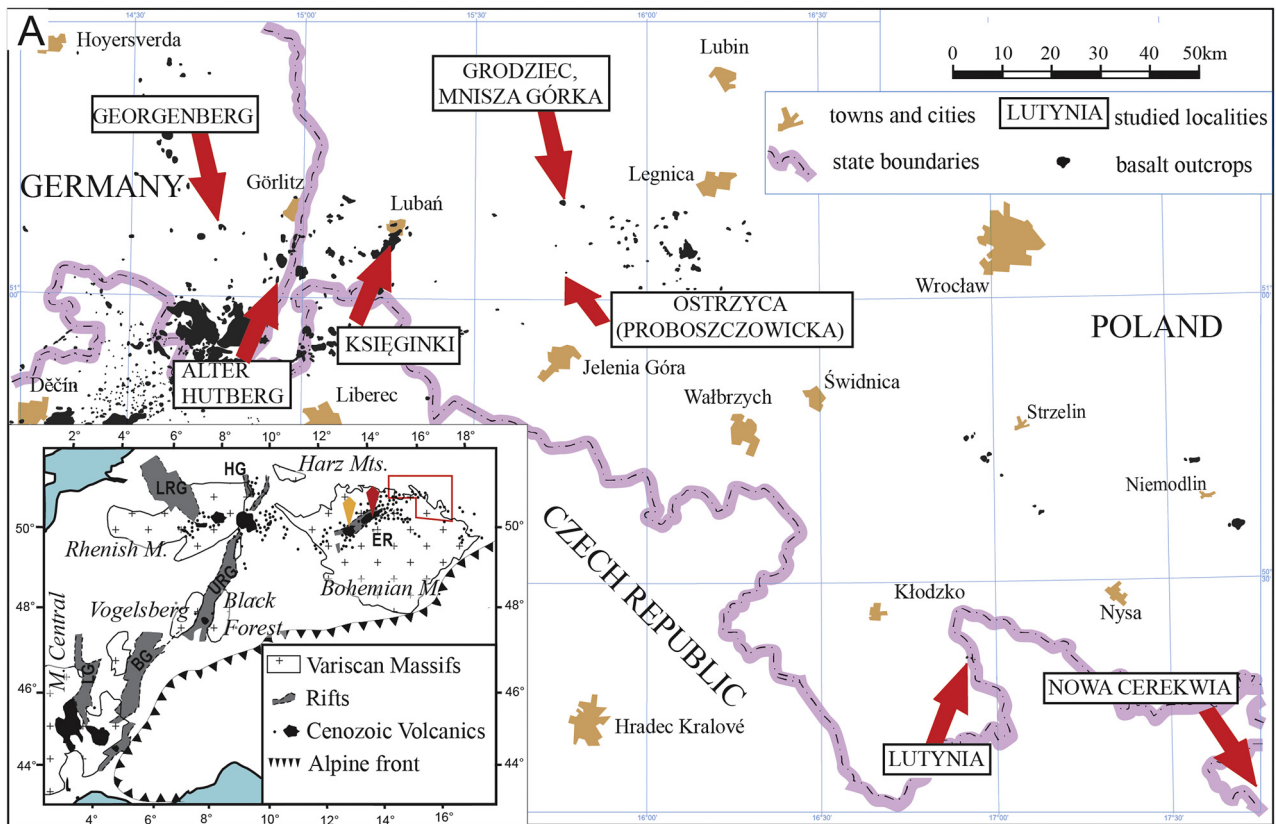
The Cenozoic lavas in Lusatia and Lower Silesia form the Lusatian Volcanic Field (located on the NE prolongation of the Ohře Rift, Büchner et al., 2015) and four "volcanic complexes" of smaller extent (Puziewicz et al., 2015). From west to east these are: Złotoryja-Jawor, Niemcza-Strzelin, Łądek Zdrój and Niemodlin, which are situated in the Labe-Odra fault system; single outcrops occur outside those complexes. The volcanic activity culminated in late Eocene-Oligocene (34.0–26.0 Ma) and early Miocene (22.0–18.0 Ma) with subordinate late Miocene-Pliocene-Pleistocene eruptions (5.5–1.0 Ma; Ar/Ar dating by Büchner et al., 2015 and K–Ar dating by Pěcskay and Birkenmajer, 2013).

Mantle and lower crustal xenoliths occur in ~3% of the localities of mafic volcanic rocks in Poland (Matusiak-Matek et al., 2017a). Locally, they are accompanied by megacrysts of clinopyroxene, in some localities megacrysts of olivine, amphibole and plagioclase are present as well; megacrysts may occur also in lavas lacking xenoliths. Megacrysts studied in this work were sampled from 8 localities (Fig. 1). The outcrops Alter Hutberg, Georgenberg and Księginki belong to the Lusatia Volcanic Field. Further east, localities Ostrzyca Proboszczowicka, Grodziec and Mnisza Górka belong to the Złotoryja-Jawor complex and locality Lutynia to the Łądek Zdrój complex. The easternmost outcrop studied of the Cenozoic volcanic rocks in Poland is Nowa Cerekwia. For the sake of brevity, we use the name Ostrzyca instead of the full name of the locality Ostrzyca Proboszczowicka.

Oligocene (32–27 Ma) lava flows from Księginki (Birkenmajer et al., 2011) are formed of nephelinite and together with the Grodziec (32.16 ± 1.37 Ma, Badura et al., 2006) nephelinitic plug and (possibly) the Ostrzyca basanite/nephelinite (Szumowska et al., 2013) represent the oldest period of volcanic activity in the area. The Lutynia basanite plug is of Pliocene age (4.56 ± 0.20 Ma; Birkenmajer and Pěcskay, 2002). In Nowa Cerekwia Upper Oligocene (26.41 ± 1.03 Ma) nephelinite lava flow was cross-cut by a Miocene (22.31 ± 0.87 Ma) plug (Badura et al., 2006). Ages of basanitic Mnisza Górka, tephritic Alter Hutberg and basanitic/nephelinitic Georgenberg (probably) lava flows (Büchner et al., 2015) remain unknown.

3. Analytical procedures

A total of 42 clinopyroxene megacrysts were studied (Table 1); trace element data from megacryst 2844 have been previously published by Puziewicz et al. (2011), thus for this sample we present only major element data. We used ~100 µm thick sections. Modal content of apatite inclusions and clinopyroxene and orthopyroxene lamellae was established on high-quality images in plane polarized light or back-scattered images with use of JMicroVison software (Rouduit, 2007). Preliminary textural and mineralogical studies were done using a Jeol JSM IT-100 scanning electron microscope equipped with an Oxford Act-X EDS system at the Institute of Geological Sciences, University of Wrocław, Poland. Major element compositions were determined using an electron microprobe (CAMECA SX-100, University of Vienna, Austria, Department of Lithospheric Research, and University of Warsaw, Poland, Institute of Geochemistry, Mineralogy and Petrology). For both machines the same analytical conditions were applied: an accelerating voltage of 15 kV, a beam current of 20 nA and a beam



diameter of 1 μm . Counting time was usually 10–20 s, counting time for Ca and NiO in olivine were increased to 40 s in order to achieve better precision of analyses. Natural silicates and synthetic oxides were applied as standards. We have analyzed 3–4 areas in each megacrysts and performed 4 analyses in each area; the analyses were taken close to each other (up to 6 μm).

Contents of trace elements were measured “in situ” on thick sections in four different laboratories; during the analyses we have avoided places enclosing small crystals of magnetite and sulfides (see below). The majority of megacrysts were studied by high-resolution magnetic sector Inductively Coupled Plasma Mass Spectrometry (ICP-MS), using an ELEMENT 2 (ThermoFisher Scientific) with New Wave UP213 laser ablation system (Czech Academy of Science, Prague, Czech Republic, Institute of Geology). A beam diameter of 80 μm and a frequency equal to 20 Hz were used. We have used CaO as internal standard, NIST 612 glass as a primary external standard and BCR-2G glass as a secondary external standard; precision of $\pm 11\%$ for most of the elements was achieved. At the Polish Academy of Sciences, Cracow, Poland (Institute of Geological Sciences) trace elements contents were established using a XSeriesII ThermoElectron ICP-MS connected with a Resonetics RESOLUTION50 excimer laser (ArF, Müller et al., 2009). The analyses were performed using the spot size of 155 μm and a frequency of 10 Hz. The CaO content was used as internal standard, the NIST612 glass was used as a primary external standard whereas GOR 128-G was used as a secondary standard. Precision of $\pm 1\text{--}6\%$ for most of the elements, $\pm 10\%$ for Y, Nb, Ta and $\pm 16\%$ for Zr was achieved. At the Observatoire Midi Pyrénées, University Toulouse III, France, the trace element concentrations were determined with Agilent 7500 ICP-MS instrument coupled either to a CETAC laser ablation module that uses a 266 nm frequency-quadrupled Nd-YAG laser or to a commercial femtosecond Ti:Sa laser system (Amplitude Technologies Pulsar 10) based on the chirped-pulse amplification (CPA) technique. A beam diameter of 50–100 μm and a frequency of 10 Hz were used, precision was 1–10% (details in Puziewicz et al., 2011). The CaO content was used as internal standard, NIST 612 and NIST 610 glasses were used as primary and secondary external standards, respectively. Megacryst MM76 containing orthopyroxene lamellae was analyzed with a Thermo Scientific ELEMENT XR spectrometer coupled with an M-50 HR Resonetics laser at FIERCE in the Goethe-University in Frankfurt am Main, Germany. A beam diameter of 33 μm and a frequency of 8 Hz were used. The SiO₂ content was used as internal standard, NIST612 and BIR-1 glasses were used as primary and secondary external standards, respectively. The precision is $\pm 5\%$. Although the beam used in this sample was 33 μm and the ablation spots were placed in the middle of lamellae, some contamination was unavoidable as the laser intersected narrowly spaced lamellae boundaries. Therefore, during data processing we have used the signal from Ca and Mg, which were monitored along with trace elements, as a discrimination tool between pure and contaminated analyses. Comparison of the results made on megacryst MM76 in laboratories in Toulouse and Frankfurt showed that the data from the first laboratory are 10–29% higher, only for Pb the differences were more significant and reached 300%. As megacryst MM76 is the most depleted in trace elements (see the following text), resulting in greater analytical uncertainty, the above reported variations between results from different laboratories are taken to be maxima. In the following text data from Frankfurt was used for sample MM76.

Ferric iron contents were determined for 10 samples by ⁵⁷Fe Mössbauer spectroscopy at the Goethe-University Frankfurt, Germany. Sample material was drilled out of each megacryst and ground into a fine powder. A sufficient amount of the sample was used to prepare an

absorber thickness of $\sim 5 \text{ mg Fe cm}^{-2}$ to avoid potential saturation effects. Samples were mixed together with a small amount of sugar (Fe-free filler), packed into a 6 mm diameter hole in a 1 mm thick Pb disc and closed off with tape on both sides. To improve the signal to noise ratio, a Ta-foil with a hole of appropriate diameter was attached to the sample holder to reduce errant gamma rays reaching the detector. Spectra were obtained at room temperature in transmission mode using a constant acceleration Mössbauer spectrometer with a nominal 50 mCi ⁵⁷Co source in a 6 μm Rh matrix. The velocity scale was calibrated relative to 25- μm -thick $\alpha\text{-Fe}$ foil using the positions certified by NIST. Mirror image spectra were collected over 512 channels with a velocity range of $\pm 5 \text{ mm/s}$.

The NORMOS software package (distributed by Wissenschaftliche Elektronik GmbH, Germany) was used to fit the spectra. Spectra are composed of two broad absorption peaks which were fit following the approach by Woodland et al. (2006). The spectral model employed for clinopyroxene consisted of two quadrupole split doublets for Fe²⁺ and one doublet for Fe³⁺, each with Lorentzian peak shapes and equal areas. The individual peak widths were allowed to vary for the Fe²⁺ doublets in order to account for next nearest neighbour effects. Hyperfine parameters for the subspectra as well as Fe³⁺/ΣFe are given in Electronic Table A1. Uncertainties in Fe³⁺/ΣFe are considered to be ± 0.01 (Woodland et al., 2006).

The megacryst sample digestion for Sr and Nd isotopic analyses were carried out using a mixture of ultra-pure HF/HNO₃ (5:1) in Savillex™ beakers for three weeks at 100–150 °C on a hot plate. The residue, after evaporation of the acids, was repeatedly treated with 5.8 N HCl until the solution became transparent. The procedure for isolation of Rb, Sr, Sm and Nd followed the standard procedure described by Thöni et al. (2008). After chemical separation, samples were analyzed on the ThermoFinnigan® Triton TI TIMS at the Laboratory of Geochronology, Department of Lithospheric Research, University of Vienna, Austria. Blanks were < 50 pg for both Nd and Sm and < 1 ng for Sr. During the period of measurement, standard values were: ⁸⁷Sr/⁸⁶Sr = 0.710270 ± 0.000007 ($n = 8$) for NBS987 and ¹⁴³Nd/¹⁴⁴Nd = 0.511842 ± 0.000032 ($n = 8$) for La Jolla international standards. Unfortunately, the low Sr abundance in clinopyroxene MM76 precluded acquisition of accurate and precise ⁸⁷Sr/⁸⁶Sr ratios by laser ablation ICPMS.

We used pyroxenes nomenclature after Morimoto (1989). Mg# is defined as atomic Mg/(Mg + Fe^{tot}) ratio in formula unit. Abbreviations used in text: a.p.f.u. – atoms per formula unit, wt% – weight percent, PPL – plane polarized light, BSE – backscattered electrons, PM – primitive mantle.

4. Petrography

We define the megacrysts as monocrystals whose size significantly exceeds the size of the matrix of the volcanic rock, i.e. are clearly visible in the rock with unaided eye; this rough criterion means that the smallest crystals classified as megacrysts are $\sim 0.8 \text{ cm}$ long. Clinopyroxene phenocrysts of microscopic appearance resembling that of megacrysts occur in some of the volcanic rocks (e.g. greenish clinopyroxene in Georgenberg), but, as they did not meet the macroscopic criterion, they were not analyzed in this study.

All of the megacrysts (0.8- < 4 cm, usually 1.5–3 cm long; Table 1) are macroscopically black to dark green and have subhedral shapes with single crystal faces. The crystals may be either elongated or tabular, but their edges are always rounded. In

Fig. 1. Map showing: (A) the localities of clinopyroxene megacrysts and occurrences of Cenozoic basaltic volcanic rocks in E Germany and SW Poland (compiled from Sawicki, 1995), and (B) geology of the studied area and neighboring areas (compiled from www.europe-geology.eu). Inset in A shows the studied area (red square) relative to the major tectonic units, European Cenozoic Rift System and associated Variscan Massifs; BG – Bresse Graben, ER – Eger Rift, HG – Hesse Graben, LG – Limagne Graben, URG – Upper Rhine Graben (Ulrych et al., 2011); red diamond point České Středohoří Volcanic Complex and approximate localization of Dobkovičky quarry (Ackerman et al., 2012); orange diamond points Doupovský hory Volcanic Complex.

Table 1
Textural features of the clinopyroxene megacrysts.

Locality	No. of samples	Group	Sample names	Petrographic features
Lutynia	11	MMg#/HMg#	L25A, L25B, L32, L32B, LB1, LB3, Lu2.09, Lu3.09, 2911B, 2561/MM76	1.5 cm - 4 cm long, transparent to light greyish, spongy rims, scarce minute inclusions of opaque minerals ordered in lines/ orthopyroxene lamellae
Księginki	6	MMg#	2475, 2477, 2484, 2523, 2844, 2869	2- < 3 cm long, transparent to greyish, spongy rims, numerous minute inclusions of opaque minerals ordered in square sectors, scarce olivine inclusions
Nowa Cerekwia	1	MMg#	NC3a	1 cm long, grey, recrystallization rim, spongy along cracks
Alter Hutberg	7	MMg#	3338, 3339-2a, 3340-2a, 3341-1-2, 3341-2a, 3341-2b, 3341-2, 3342	1.5-3 cm long, grey, recrystallization rims, very scarce olivine and minute opaque mineral inclusions, secondary carbonate inclusions
Georgenberg	10	LMg#	3311, 3313, 3314, 3315a, 3315b, 3317, 3318a, 3318b, 3318c, 3319a	1-4 cm long, greyish to grey, recrystallization rims, often large inclusions of opaque minerals, scarce ordered minute opaque minerals and very scarce apatite inclusions, secondary carbonates inclusions, newly crystallized rims
Mnisza Górka	3	LMg#	GM16, GM27, GM28	1.5-1.7 cm long, green, newly crystallized rims
Grodziec	2	LMg#	Gro23A, Gro23C	0.8-2.5 cm long, green, locally spongy, newly crystallized rims
Ostrzyca	2	LMg#	OS3, OS4	1.2-1.7 cm long, green, scarce to abundant apatite inclusions, newly crystallized rims

Georgenberg clinopyroxene megacrysts enclose 0.5–1.5 cm long, oval aggregates of fine clinopyroxene, olivine, alkali feldspar/glass, rhönite and ilmenite (Fig. 2A).

Crystals from Księginki and Lutynia are formed of transparent to greyish cores and spongy rims (Fig. 2B), which in extreme cases may be as thick as 1.1 cm. Megacrysts from Alter Hutberg, Georgenberg and Nowa Cerekwia are homogeneously grey to brownish in plane polarized light (Fig. 2C). Crystals from Mnisza Górka, Grodziec, and Ostrzyca are intensely green and show sector zoning (Fig. 2D). Contact with the host rock is usually sharp, but megacrysts with well-defined colours are necklaced by a yellowish, ~10 µm wide zone of newly crystallized clinopyroxene (Lipa et al., 2014); the boundary between coloured core and the rim is sharp (Fig. 2D). Elongated to oval inclusions of magnetite and sulfides (20 to 70 µm in diameter) are present in some of the megacrysts from Lutynia, Księginki and Georgenberg (Table 1). They are arranged in parallel, three-dimensional streaks covering either entire core or forming well defined clusters (Fig. 2B, E); the streaks of opaque minerals are not related to any visible discontinuities or cracks in megacrysts. The megacryst MM76 from Lutynia contains lamellae of orthopyroxene (Fig. 2F) constituting 42.3 vol% of the megacryst. Oval inclusions of partly iddingsitised olivine (1–7 mm long) are present in some of the megacrysts from Alter Hutberg and Księginki (Fig. 2G), while those from Georgenberg often enclose (1–3 mm) long subhedral crystals of magnetite (Fig. 2C). Small (100–500 µm) inclusions of apatite are present in some samples from Ostrzyca and Georgenberg; the modal content of apatite inclusions (where present) in the megacryst set from Ostrzyca (Lipa et al., 2014) is 3 to 12 vol%, in the samples studied here it is only 0.5 vol%. Carbonates occur along cracks and in voids in coloured megacrysts (Fig. 2C, D, G); in some of the carbonates well-defined banding is visible, but most of the inclusions are texturally homogeneous.

5. Major and trace element chemistry of clinopyroxene megacrysts and their inclusions

The studied clinopyroxene megacrysts are usually chemically homogeneous; the only samples where slight chemical heterogeneity in terms of Mg# and trace element contents appears are GM28, OS3 and OS4 (Table 1). Composition of the megacryst may vary close to cracks and spongy areas. We have divided them into three groups on the basis of their Mg#:

- (1) high Mg# (Mg# = 91.09–91.52; hereafter “HMg#”);
- (2) medium Mg# (Mg# = 76.8–83.4; “MMg#”);
- (3) low Mg# (Mg# = 62.2–74.6; “LMg#”).

Megacrysts from one locality usually belong to one group, only in Lutynia crystals from groups HMg# and MMg# occur. The HMg# group comprises only one megacryst (MM76) which is an Al–Cr diopside ($\text{Al}_2\text{O}_3 = 6.30\text{--}7.18$ wt%, $\text{Cr}_2\text{O}_3 = 0.68\text{--}0.72$ wt%) with $\text{Fe}^{3+}/\Sigma\text{Fe}$ ratio of 0.51 (Fig. 3A, B, C; Table 2, Electronic Tables A2, A3). This megacryst is characterized by an extremely low TiO_2 content (0.08–0.16 wt%).

The MMg# megacrysts suite comprises samples from Księginki, Lutynia, Nowa Cerekwia and Alter Hutberg. The MMg# crystals from Lutynia and Księginki have usually composition of Al–Ti augite ($\text{Al}_2\text{O}_3 = 7.07\text{--}9.13$ wt%, $\text{TiO}_2 = 0.60\text{--}1.89$ wt%) with scarce transitions to diopside and are relatively CaO-poor (usually from 16.00 to 21.30 wt %) and Cr_2O_3 -poor (0.00–0.21 wt% only in one sample 0.48 wt%); their $\text{Fe}^{3+}/\Sigma\text{Fe}$ ratio ranges from 0.14 to 0.36. The MMg# megacrysts from Nowa Cerekwia and Alter Hutberg are an Al–Ti diopsides ($\text{Al}_2\text{O}_3 = 5.70\text{--}9.38$ wt%, $\text{TiO}_2 = 1.27\text{--}2.58$ wt%), those from Alter Hutberg being mostly subsilicic (Fig. 3A, B, C). They contain 20.42–22.70 wt% of CaO and their $\text{Fe}^{3+}/\Sigma\text{Fe}$ ratio ranges from 0.50 to 0.66 (Fig. 3E; Table 2, Electronic Tables A2, A3). Their Cr_2O_3 content does not exceed 0.34 wt%.

The LMg# megacrysts (Georgenberg, Ostrzyca, Mnisza Górka, and Grodziec) have compositions of Al–Ti diopside; those from Georgenberg ($\text{Al}_2\text{O}_3 = 7.10\text{--}10.21$ wt%, $\text{TiO}_2 = 1.95\text{--}3.20$ wt%) being all subsilicic and often calcic ($\text{CaO} = 22.20\text{--}22.83$ wt%), while megacrysts from the other three localities ($\text{Al}_2\text{O}_3 = 2.83\text{--}6.05$ wt%, $\text{TiO}_2 = 0.66\text{--}1.96$ wt%) commonly have slightly higher Na_2O contents ($\text{Na}_2\text{O} = 0.74\text{--}1.72$ wt% vs. 0.45–0.96 wt%; Fig. 3 D). All the LMg# megacrysts are Cr_2O_3 -poor (<0.06 wt%). As expected, all megacrysts exhibit a negative correlation between Na_2O and CaO contents, but in the LMg# suite, the latter is less variable (Fig. 3E). The $\text{Fe}^{3+}/\Sigma\text{Fe}$ ratio of LMg# megacrysts is 0.407–0.564 (Electronic Table A3).

Chondrite-normalized trace elements patterns from almost all of the megacrysts are similar, however the absolute concentrations vary widely (Table 2, Electronic Table A4). The incompatible trace elements concentrations increase with decreasing Mg#, the only exceptions are Th and U contents which do not follow the negative trends (Fig. 4). On the other hand, amount of Zr, Hf and Sr in LMg# megacryst from Ostrzyca, Mnisza Górka (and partly Grodziec) is higher than in the other megacrysts with similar Mg#. The megacrysts are mostly Light Rare Earth Elements (LREE) - enriched relative to Heavy REE (HREE; $\text{Ce}_N/\text{Lu}_N = 2.41\text{--}9.52$) with convex downward REE patterns (Fig. 5A, B); only the HMg# sample from Lutynia is LREE depleted ($\text{Ce}_N/\text{Lu}_N = 0.02$). All the megacrysts have a distinct negative Pb anomaly and Rb, Ba, Th and U contents below primitive mantle level (Fig. 5 C, D). In megacrysts from Ostrzyca and Mnisza Górka positive Zr–Hf anomalies occur.

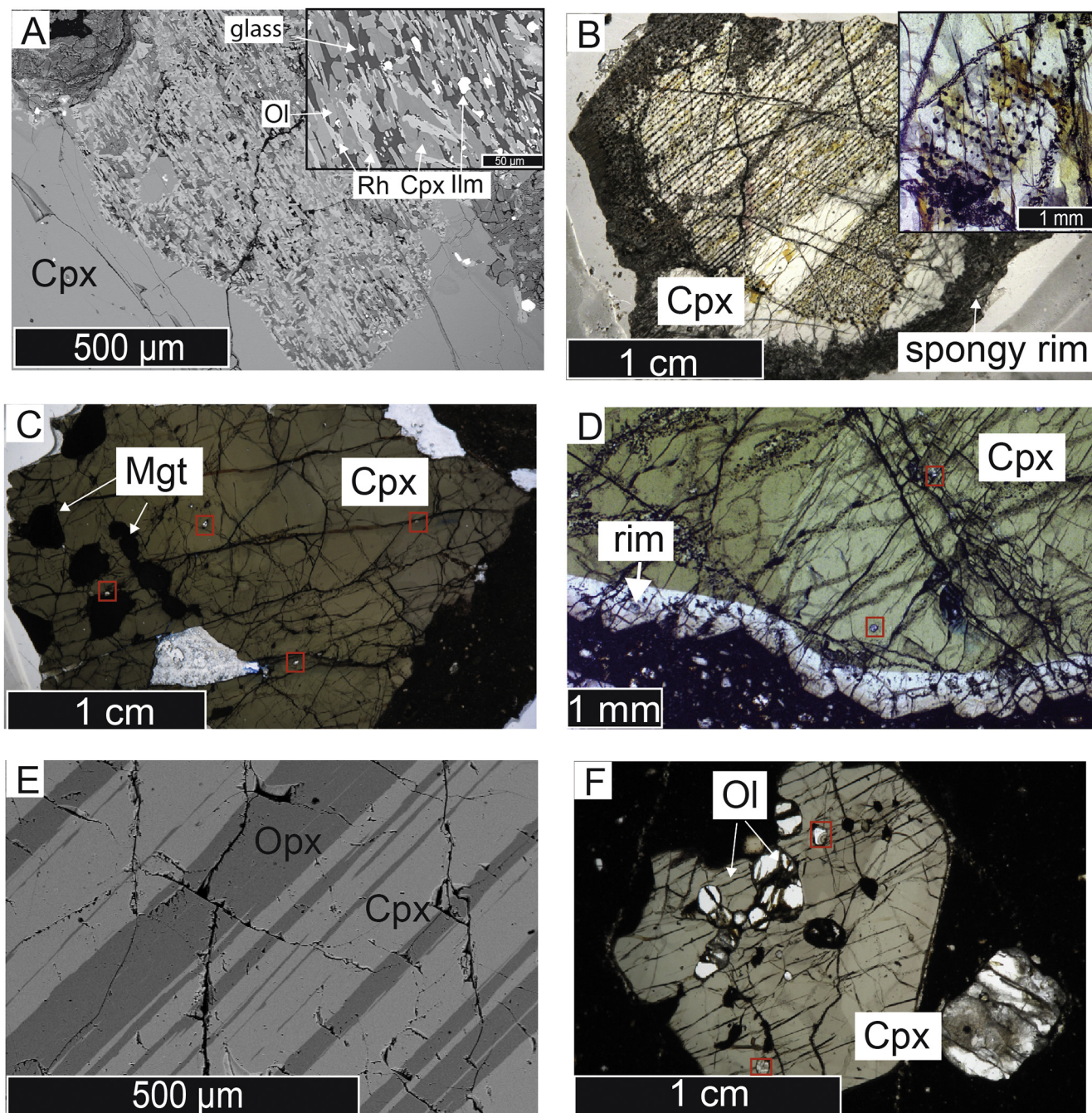


Fig. 2. Textural features of clinopyroxene megacrysts: A - fine-grained aggregate in megacryst from Georgenberg; inset shows enlargement of the structure (sample 3314, BSE image; Cpx – clinopyroxene, Ol – olivine, Rh – rhönite, Ilm – ilmenite); B – megacryst 2524 from Księginki; core of the crystal is interspersed by streaks of minute inclusions of sulfides and magnetite (PPL); inset shows cluster formed of oval crystals of magnetite and sulfides (Księginki 2869); C - megacrysts 3819a from Georgenberg with inclusions of magnetite (PPL); D - rim of newly crystallized clinopyroxene on megacryst OS3 from Ostrzyca (PPL); E - Cpx-Opx lamellae in megacryst MM76 (Lutynia, BSE); F - olivine inclusion in megacryst 3340-2a, Alter Hutberg (PPL). Red squares point out some of the inclusions of carbonates.

Opaque minerals forming small inclusions in clinopyroxene are magnetite (with transitions to spinel) and pyrite ($\pm\text{Cu}$, $\pm\text{Ni}$) in Lutynia and Księginki (MMg#) and pyrrhotite in Georgenberg megacrysts (Electronic Tables A5 and A6). Sulfides from MMg# megacrysts are characterized by $\text{Ni}/(\text{Ni} + \text{Fe}) = 0.11$, whereas in LMg# ones the ratio is ≤ 0.02 . Large inclusions of opaque minerals in Georgenberg LMg# megacrysts are titanomagnetite ($\text{TiO}_2 = 13.29\text{--}16.41$ wt% corresponding to 0.36–0.45 atoms of Ti p.f.u.).

Olivine inclusions in MMg# crystals have 79.05 to 83.75 mol% Fo and 0.08–0.14 wt% NiO (Electronic Table A7). The Ca content in

olivine is constant within a sample and varies from 1600 to 3300 ppm within the entire megacryst suite. Lamellar orthopyroxene from HMg# megacryst from Lutynia (Al–Cr enstatite; $\text{Al}_2\text{O}_3 = 5.56\text{--}6.78$ wt%) has a Mg# = ~ 0.91 ; it is LREE-depleted ($\text{Ce}_N/\text{Lu}_N = 0.30$) and shows slight positive anomalies in Ti, Pb and Hf contents (Electronic Table A4).

Apatite from Georgenberg and Ostrzyca megacrysts has the composition of hydroxyl-apatite (Electronic Table A8, Lipa et al., 2014). Apatite from Georgenberg is strongly enriched in LREE ($\text{La}_N/\text{Lu}_N = 37.41\text{--}41.50$), characterized by negative Pb and Zr–Hf anomalies, and

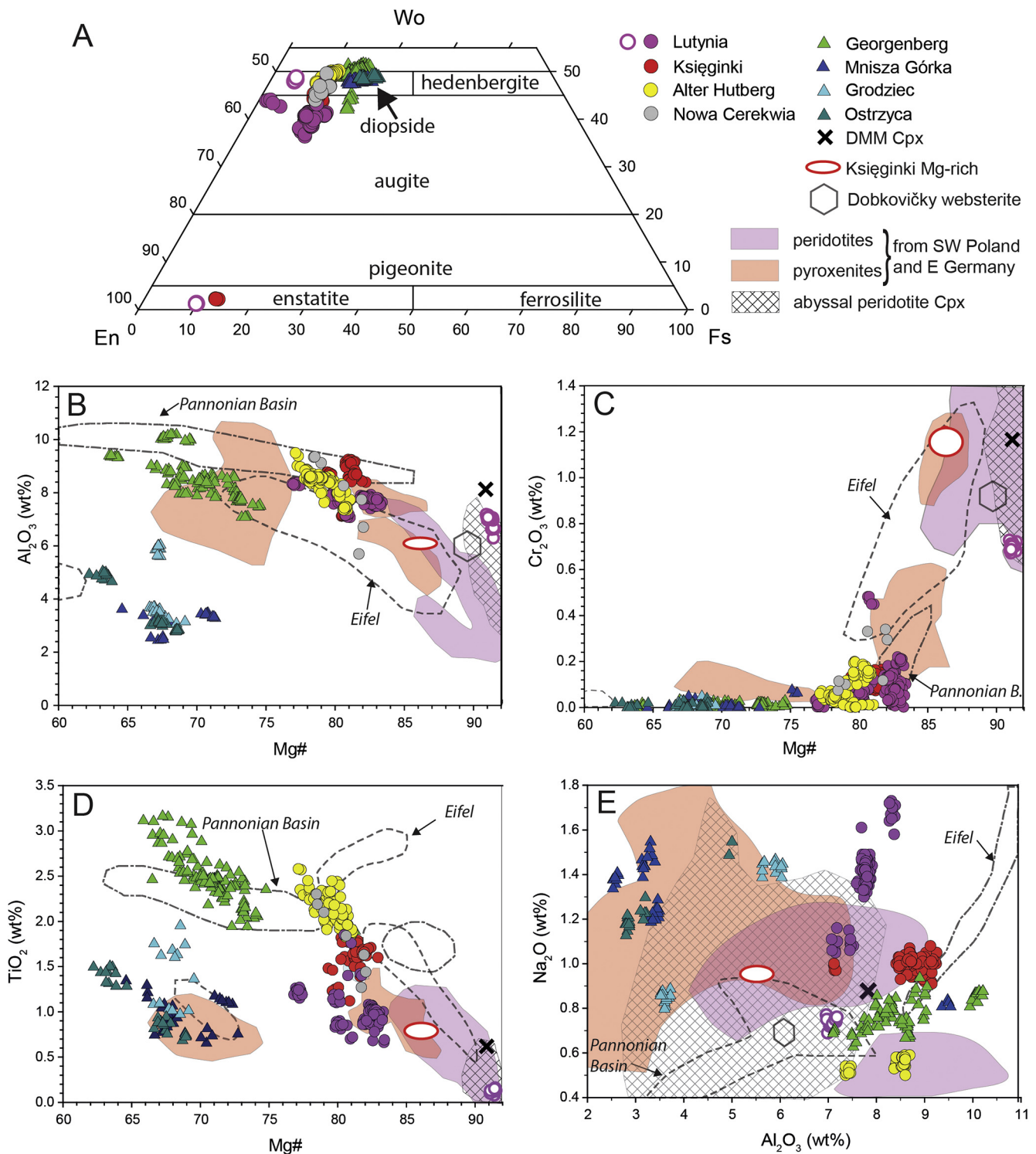


Fig. 3. Compositional variations between clinopyroxene megacrysts: A – Fs-Wo-En pyroxene classification diagram; B – Mg# versus Al_2O_3 contents; C – Mg# versus Cr_2O_3 contents; D – Mg# versus TiO_2 ; E – CaO versus Na_2O contents. Open symbols show the HMg# megacryst. For comparison data from pyroxenitic and peridotitic xenoliths from SW Poland and E Germany (Matusiak-Matek et al. (2017a, 2017b), Matusiak-Matek et al., 2010; Kukuła et al., 2015; Puziewicz et al., 2011 and authors' unpublished data) are shown; data for xenoliths from Dobkovičky after Ackerman et al. (2012), for megacrysts from Eifel after Shaw and Eyzaguirre (2000), for megacrysts from Pannonian Basin after Dobosi and Jenner (1999) and for Mg-rich megacryst from Księginiki (Puziewicz et al., 2011) are also indicated. Composition of clinopyroxene forming DMM (Depleted MORB Mantle) after Workman and Hart (2005) and composition of clinopyroxene from clinopyroxene from abyssal peridotites after Warren (2016).

contains 93 ppm of Th and 46 ppm of U (Fig. 4). Apatite from Ostrzyca (Lipa et al., 2014) is richer in most trace elements, but shows the same general characteristic. It belongs to “group B” apatites defined by O'Reilly and Griffin (2000).

6. Isotopic composition

The $^{87}\text{Sr}/^{86}\text{Sr}$ ratios in megacrysts from Księginiki vary from 0.703323 to 0.703496 and $^{143}\text{Nd}/^{144}\text{Nd}$ reach the values 0.512890–0.512904

Table 2
Chemical features of clinopyroxene forming megacrysts.

Locality	Cpx classification ^{a,b}	Group	Mg# Cpx ^b	Cr ₂ O ₃ Cpx (wt%) ^b	Na ₂ O Cpx (wt%) ^b	Al ^{IV} (a.pfu)	Al ^{VI} (a.pfu)	total REE (ppm) ^b
Lutynia	Ti-Al (±Cr) augite/Al-Cr augite	MMg#	76.81–83.40/91.09–91.52	0.00–0.61/0.68–0.72	0.46–1.80/0.71–0.83	0.15–0.20/0.13–0.16	0.13–0.20/0.13–0.16	17.28–31.13/4.43
Księginki	Al-Ti augite	MMg#	79.31–82.93	0.01–0.17	0.87–1.13	0.17–0.24	0.12–0.17	27.30–39.07
Nowa Cerekwia	Al-Cr diopside	MMg#	80.61–82.04	0.12–0.34	0.78–0.90	0.16–0.24	0.08–0.12	34.90–47.11
Alter Hutberg	(±subsilic) Ti-Al diopside	MMg#	77.14–83.41	0.02–0.54	0.45–0.62	0.24–0.31	0.08–0.11	50.00–63.50
Georgenberg	subsilic (calcic) Ti-Al augite or Ti-Al-Cr diopside	LMg#	65.85–74.77	0–0.05	0.60–0.96	0.22–0.36	0.07–0.12	44.92–101.14
Mnisza Górka	Ti-Al diopside	LMg#	64.59–72.73	0–0.05	0.96–7.72	0.05–0.12	0.03–0.06	75.06–90.05
Grodzicz	Ti-Al diopside	LMg#	66.58–69.53	0.00–0.05	0.74–1.47	0.11–0.20	0.03–0.10	59.39–70.06
Ostrzyca	Ti-Al diopside	LMg#	62.22–68.97	0.00–0.04	1.14–1.64	0.08–0.14	0.04–0.08	61.80–88.41

Mg# = Mg/(Mg + Fe⁶⁵).

a.pfu – atoms per formula unit.

HMg# – high Mg# megacrysts.

MMg# – medium Mg# megacrysts.

LMg# – low Mg# megacrysts.

^a According to Morimoto et al. (1989).

^b Characteristic of HMg# sample is given after slash.

(Electronic Table A9; Fig. 6). In Lutynia megacrysts the ⁸⁷Sr/⁸⁶Sr ratio is 0.703291 and that of ¹⁴³Nd/¹⁴⁴Nd is 0.512903. The megacrysts from Ostrzyca are characterized by similar isotopic ratios: 0.703221–0.703226 for Sr and 0.512906–0.512911 for Nd. The isotopic ratios place the megacrysts close to the HIMU field and close to Cenozoic volcanic rocks from Lower Silesia (Fig. 6).

7. Pressure and temperature of megacrysts formation

The majority of geothermobarometers establish P-T conditions of chemical equilibrium between two or more phases, but clinopyroxene megacrysts are usually monocrystalline and it is uncertain if they are in equilibrium with the surrounding lava. However, Nimis and Taylor (2000), Nimis and Ulmer (1998) and Putirka (2008) have calibrated algorithms based solely on the composition of clinopyroxene that is implicitly in equilibrium with a mafic (basaltic) melt. In these cases, the derived conditions of crystallization are subject to significant error, especially at very low pressures. However, it is considered that differences observed between samples from the same lava unit or between locations with similar whole-rock chemistry should be meaningful in terms of relative depths of crystallization.

7.1. Temperature

To estimate temperatures of formation of the clinopyroxene megacrysts we have used the clinopyroxene-based geothermometer by Nimis and Taylor (2000) with corrections by Putirka (2008), eq. 32d). As this geothermometer is pressure-dependent, we have iteratively calculated temperature by coupling the result of eq. 32d with the pressure calculated from eq. 32a from Putirka (2008). Calculation of temperature (as well as pressure) of crystallization of megacrysts from Ostrzyca was not possible due to their heterogeneous chemical composition.

The highest temperatures are recorded by the MMg# megacrysts from Lutynia (1327–1359 °C, with one megacryst giving 1264 °C; Electronic table A3) and only slightly lower temperatures were calculated for the HMg# megacryst (1283 °C). Megacrysts from Księginki yield temperatures from 1231 to 1262 °C, while those from Alter Hutberg record 1122–1149 °C. For the LMg# megacrysts, calculated temperatures are generally lower (1037–1099 °C), with single megacrysts giving lower (1004 °C) or higher (1128 °C) temperatures (Electronic Table A3).

In the studied suite of megacrysts, orthopyroxene is present as exsolution lamellae in the HMg# sample from Lutynia (MM76). The presence of lamellae points to relatively slow cooling, allowing enough time for exsolution to occur. To calculate the temperature of exsolution between the two phases we have used geothermometers based on major-element and trace-element equilibrium between clinopyroxene and orthopyroxene (Brey and Köhler, 1990 and Liang et al., 2013, respectively). The calculated temperatures of equilibration vary from 894 to 927 °C (Brey and Köhler, 1990; assumed pressure 0.11 GPa) to 1009 ± 20 °C (Liang et al., 2013).

7.2. Pressure

To estimate the pressure conditions of crystallization of megacrysts, we have used two geobarometers, one by Nimis and Ulmer (1998) and the other by Putirka (2008); eq. 32a). The geobarometer established by Nimis and Ulmer (1998) for clinopyroxene in equilibrium with a basaltic liquid is essentially an inversion of single-crystal crystallographic data in terms of a number of chemical components. As this included the separate effects of Fe³⁺ and Fe²⁺ occupancies, knowledge of Fe³⁺/ΣFe is required. Thus, Fe³⁺ contents of a subset of clinopyroxene megacrysts was determined by combining Fe³⁺/ΣFe measurements by Mössbauer spectroscopy along with total Fe cation contents derived from electron microprobe analyses. For the remaining samples, the Fe³⁺/ΣFe was calculated from mineral chemical composition by charge

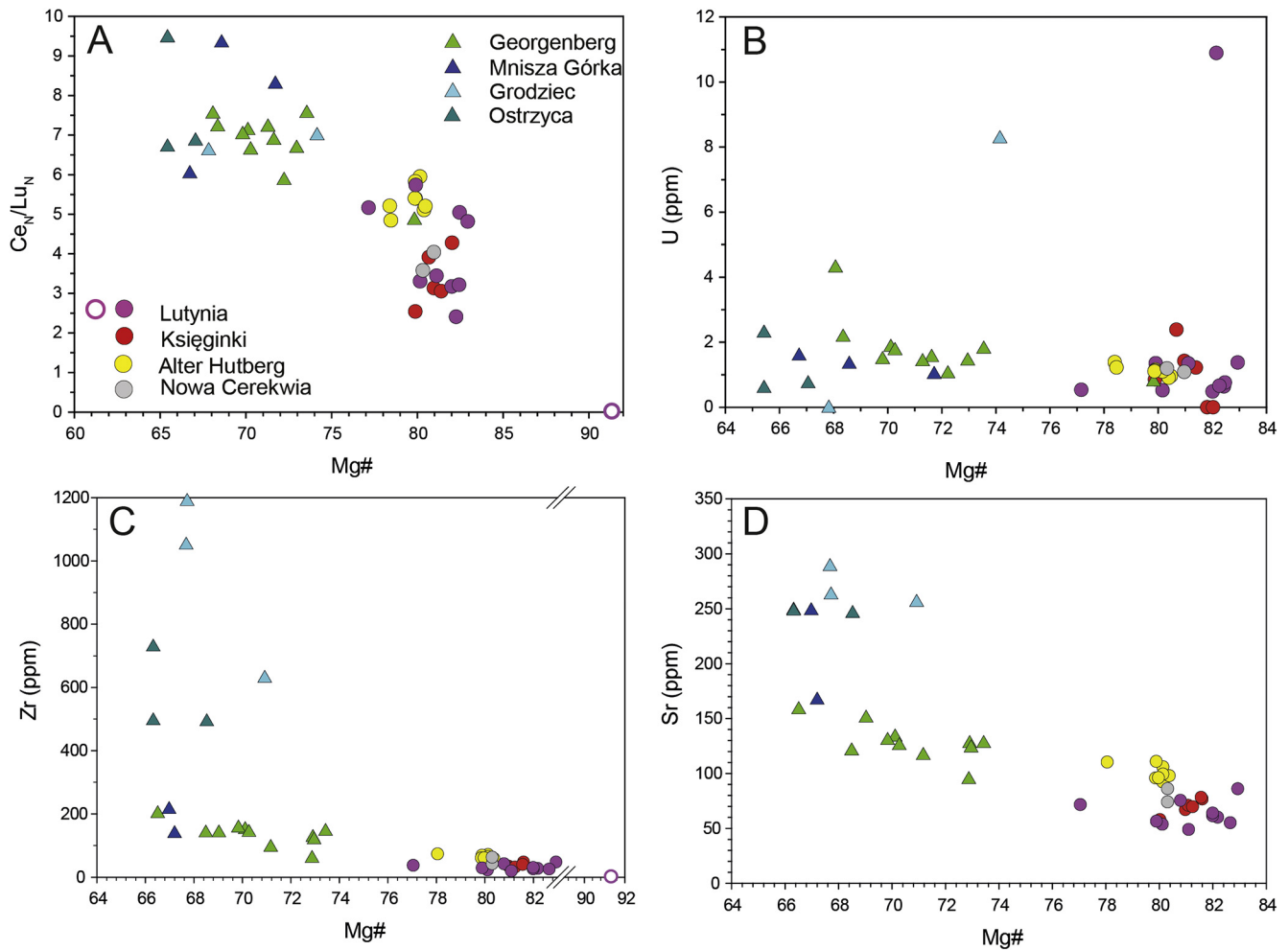


Fig. 4. Relations between Mg# and trace elements in megacrysts A - Mg# vs. chondrite-normalized Ce/Lu ratios; B - Mg# vs. U content; C - Mg# vs. Zr content; D - Mg# vs. Sr content.

balance (Electronic Table A3). However, from the assessment of Canil and O'Neill (1996) for mantle-derived clinopyroxene we are aware of a possible much greater uncertainty in $\text{Fe}^{3+}/\Sigma\text{Fe}$ estimates derived by stoichiometric calculation. Because of the small number of samples measured by Mössbauer spectroscopy ($n = 7$), any interpretation of a pressure-effect on the $\text{Fe}^{3+}/\Sigma\text{Fe}$ of our clinopyroxene megacrysts would be premature.

Using the Nimis and Ulmer (1998) we have also iteratively calculated the pressure coupled with the temperature derived from eq. 32a of Putirka (2008). The highest pressures of formation are recorded in the MMg# megacrysts from Lutynia: 2.1–2.3 GPa (in one sample 1.5 GPa; Putirka (2008)) and 0.9–1.4 GPa (Nimis and Ulmer, 1998; Electronic Table A3). Pressures of formation of megacrysts from Księginki are 1.3–1.4 GPa and 0.8–1.1 GPa, respectively. Surprisingly, the HMg# megacryst from Lutynia records lower pressures (0.8–1.3 GPa) than the MMg# megacryst from the same locality. Megacrysts from localities different than Lutynia and Księginki were formed under similar pressures, those calculated with Putirka (2008) algorithm are 0.3–1.1 GPa, and the Nimis and Ulmer (1998) method gave values from 0.4 to 1.1 GPa (Electronic Table A3).

Pressures calculated with the two methods are generally in good agreement, but with systematically lower pressures obtained from the Nimis and Ulmer (1998) model. The correlation coefficient is $R^2 = 0.76$, but if results for MMg# megacrysts from Lutynia are omitted, the R^2 increases to 0.80 (Fig. 7A). The pressures calculated for Lutynia MMg# megacrysts usually exceed 2 GPa; such high pressures

of megacryst formation are typical for megacrysts from kimberlites (e.g. Bussweiler et al., 2018; Ashchepkov, 2011; Kostrovitsky et al., 2004), but only scarcely reported from alkaline volcanics (Rankenburg et al., 2004; Roberts et al., 2019) and thus should be treated with caution. The elevated pressures could result from discrete heterogeneities in chemical composition of megacrysts (Hammer et al., 2016), but the pressure estimations in the MMg# megacryst from Lutynia were homogenous within a sample (Relative Standard Deviation = 0.00–0.05 with the suite). Mollo et al. (2013) showed that high cooling rates may result in disequilibrium partitioning of some elements into fast-growing crystals – Al, Na and Ti preferentially enter clinopyroxene, while partitioning of Si, Ca and Mg decreases with increasing cooling rate. In the problematic samples from Lutynia, a strong positive correlation between Al_2O_3 and Na_2O contents occurs, pointing their common partitioning into megacryst (Fig. 3D); such relation is only weakly (if at all) visible in other megacrysts. Therefore, we suggest that the high pressures calculated for MMg# Lutynia megacrysts may not reflect their very deep origin, but rather high cooling rates and fast growth of crystals. Therefore, for this group of megacrysts, we will use the pressure estimates calculated with algorithm by Nimis and Ulmer (1998).

As the MOHO in the studied area is located at depth 31–35 km (Majdański et al., 2006) corresponding to pressures 0.8–0.9 GPa, the megacrysts from Lutynia (0.9–1.4 GPa) and Księginki (0.8–1.4 GPa) formed under mantle conditions, while megacrysts from other localities crystallized at different levels within the overlying crust (Fig. 7B).

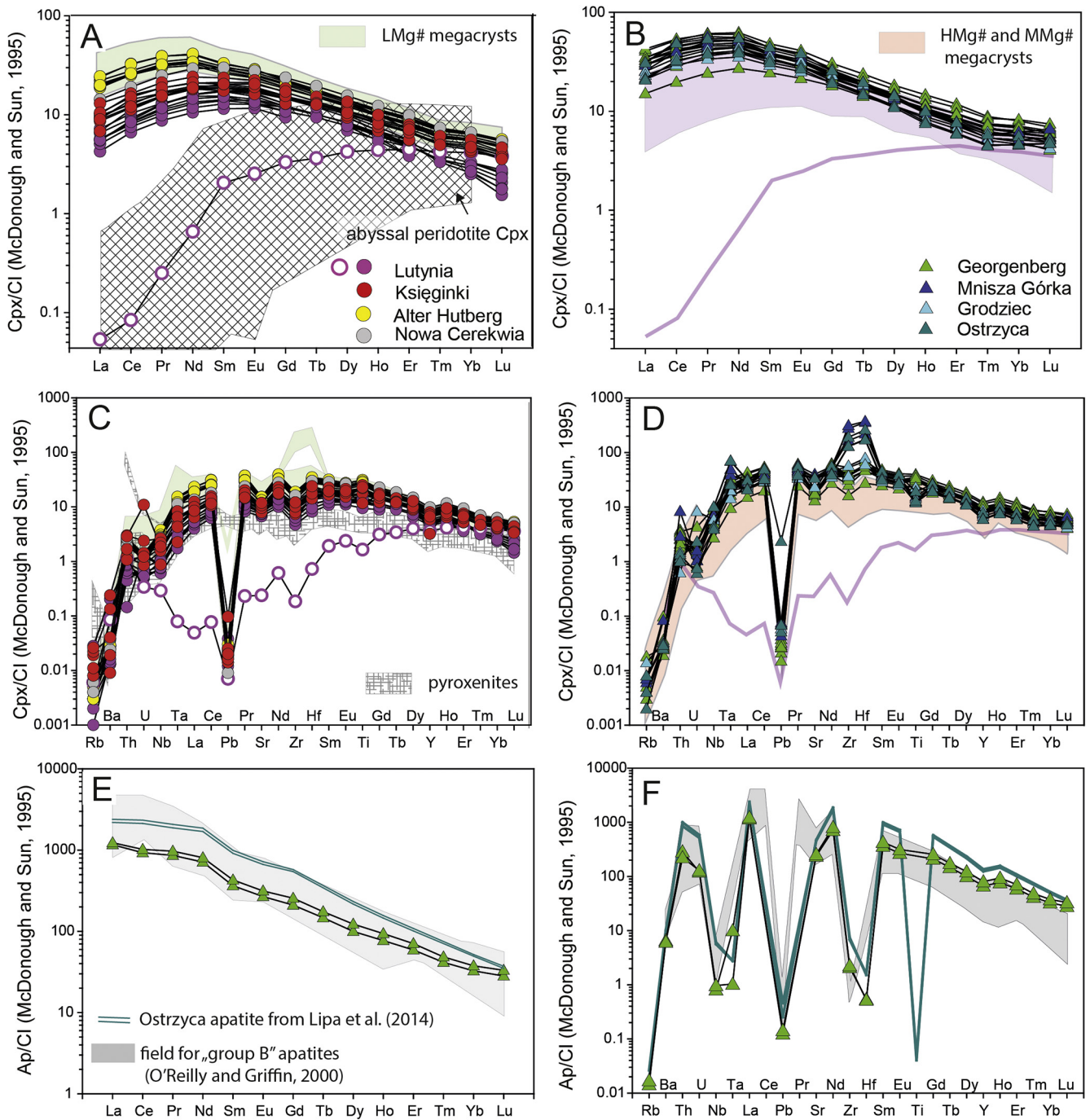


Fig. 5. Chondrite-normalized trace element composition of clinopyroxene megacrysts and apatite inclusions. A – REE diagram of HMg# and MMg# megacrysts; B – REE diagram of LMg# megacrysts; C – multi-trace elements diagram of HMg# and MMg# megacrysts; D – multi-trace elements diagram of LMg# megacrysts; E – REE diagram for apatite inclusions; F – multi-trace elements diagram for apatite inclusions. Open symbol points HMg# megacryst. Data for clinopyroxene forming abyssal peridotites after Warren (2016), data for pyroxenites from SW Poland after Matusiak-Matek et al. (2017a, 2017b), Ackerman et al., 2012 and Puziewicz et al. (2011).

8. Discussion

8.1. Origin of the megacrysts

The megacrysts of clinopyroxene may be of xenocrystic or phenocrystic/antecrystic (magmatic) origin. Xenocrystic origin from some of the sources may be excluded from the very beginning, e.g. from the studied set of localities where no plagioclase megacrysts are observed and no negative Eu anomalies in clinopyroxene occur, suggesting that plagioclase-bearing (gabbroic or more Si-saturated) pegmatites are

not the source of the megacrysts. Also, peridotitic xenoliths are likely not the source of majority of the megacrysts due to the lower Mg# and higher TiO₂, Cr₂O₃ and Al₂O₃ contents of the latter (Fig. 3).

In the following we discuss the possible origins of the megacrysts from SW Poland and SE Germany. To assess the relationship of the megacrysts to the hosts melt we have calculated the MgO/FeO ratios of hypothetical melts in equilibrium with the megacryst using the clinopyroxene–melt Fe–Mg partition coefficients values (0.25, 0.27, 0.29, 0.31, 0.31) by Putirka et al. 1996; data for Woodlark Basin; Fig. 8).

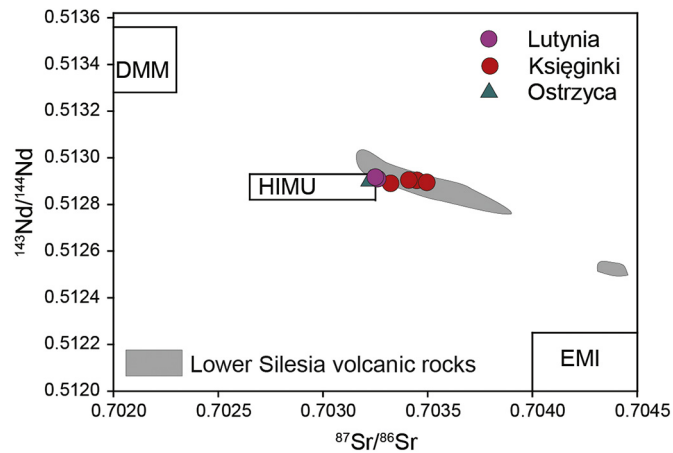


Fig. 6. $^{87}\text{Sr}/^{86}\text{Sr}$ and $^{143}\text{Nd}/^{144}\text{Nd}$ relationships in megacrysts from Lutynia, Księginki and Ostrzyca. Shaded area shows the same relationships in volcanic rocks from Lower Silesia region (Ladenberger et al., 2004; Blusztajn and Hart, 1989). Mantle end-members (EMI – Enriched Mantle I, HIMU – High- μ , DMM – Depleted MORB Mantle) after Zindler and Hart (1986).

8.1.1. Origin of the “high Mg#” megacryst

The HMg# clinopyroxene megacryst from Lutynia (MM76) differs compositionally from clinopyroxene occurring in accompanying peridotite and pyroxenite xenoliths (Fig. 3; Ackerman et al., 2012; Matusiak-Małek et al., 2010). The REE pattern of this megacryst shows LREE impoverishment relative to HREE (Fig. 5), which makes it unique in both the studied suite and the worldwide megacryst population. The MgO/FeO ratio of the hypothetical melt in equilibrium with this megacryst varies from 2.15 to 2.99, which is much higher than that of host basanite melt (1.19). Moreover, the calculated composition of melt in equilibrium with megacryst MM76 is much more LREE depleted than the host basanite (Fig. 9) and any Cenozoic mafic melt from eastern part of CEVP (Ulrych et al., 2011). Those features show unambiguously that the HMg# megacryst from Lutynia cannot be cognate with local alkaline melts (xenocryst) and its mantle origin must be considered.

The basanite from Lutynia carries numerous mantle peridotite xenoliths, usually containing LREE-enriched clinopyroxene (Matusiak-Małek et al., 2010) and the only LREE-depleted clinopyroxene (sample MM30

from Matusiak-Małek et al., 2010) differs from the HMg# megacryst in terms of major element composition ($\text{Al}_2\text{O}_3 \sim 2.05$ wt%, CaO 23.81 wt%, Mg# 94.3–94.8) and texture. On the other hand, the content of middle REE (MREE) and HREE in HMg# megacryst is identical to that of clinopyroxene from Lutynia group C peridotites (Iherzolites with clinopyroxene having convex upward REE-pattern, Op. Cit.) interpreted as distal parts of chromatographic column metasomatized cryptically by carbonatite-rich silicate melt. The HMg# megacryst could represent the protolith whose metasomatism produced all the lithologies sampled as xenoliths. In this case, however, the Al_2O_3 content in the resulting peridotitic clinopyroxene should be higher than in the protolith, which is not the case for Lutynia HMg# megacryst ($\text{Al}_2\text{O}_3 = 6.30\text{--}7.14$ wt%) and peridotites ($\text{Al}_2\text{O}_3 = 3.83\text{--}4.70$ wt%; Fig. 3). Thus, megacryst MM76 is not directly related to known mantle lithologies sampled by Lutynia basanite.

Clinopyroxene with LREE-depleted characteristics are scarce in eastern part of CEVP (e.g. Kukuła et al., 2015), but a websterite from Dobkovičky (Czechia, Fig. 1) formed of clinopyroxene with similar major (Fig. 3) and trace element compositions to that of the HMg# megacryst was described by Ackerman et al. (2012). This sample was interpreted, based on chemical composition and high ϵNd , to be related to a MORB-like parental melt. We have applied this interpretation to the HMg# megacryst. Calculations show, however, that the composition of melt in equilibrium with this sample is significantly LREE-poorer than the continental tholeiitic rocks; Boggaard and Wörner, 2003) and mid-ocean ridge basalts (Gale et al., 2013; Fig. 8). Moreover, the MgO/FeO ratio (2.15–2.99) of the hypothetical parental magma is much higher than that of tholeiitic melts (0.51–0.76 in Vogelsberg and 0.46–1.10 in MORBs, Op. Cit.) and grades toward the calculated ratios for primitive mantle (4.69; McDonough and Sun, 1995), depleted MORB mantle (4.73; Workman and Hart, 2005), but also to lower-end of the range characteristic for natural abyssal peridotites (3.43–7.00; Niu, 2004). Furthermore, the composition of the calculated melt in equilibrium with the HMg# megacryst plots between the composition of the most depleted abyssal peridotites and depleted MORB mantle (Fig. 10). The modelling suggests a possible origin of clinopyroxene which constitutes 58 vol% of the HMg# megacryst, however to establish the origin of the megacrysts in greater detail, the composition of orthopyroxene (42 vol%; Fig. 2 F) should also be taken into consideration. Therefore, we have mathematically homogenized the compositions of the HMg#

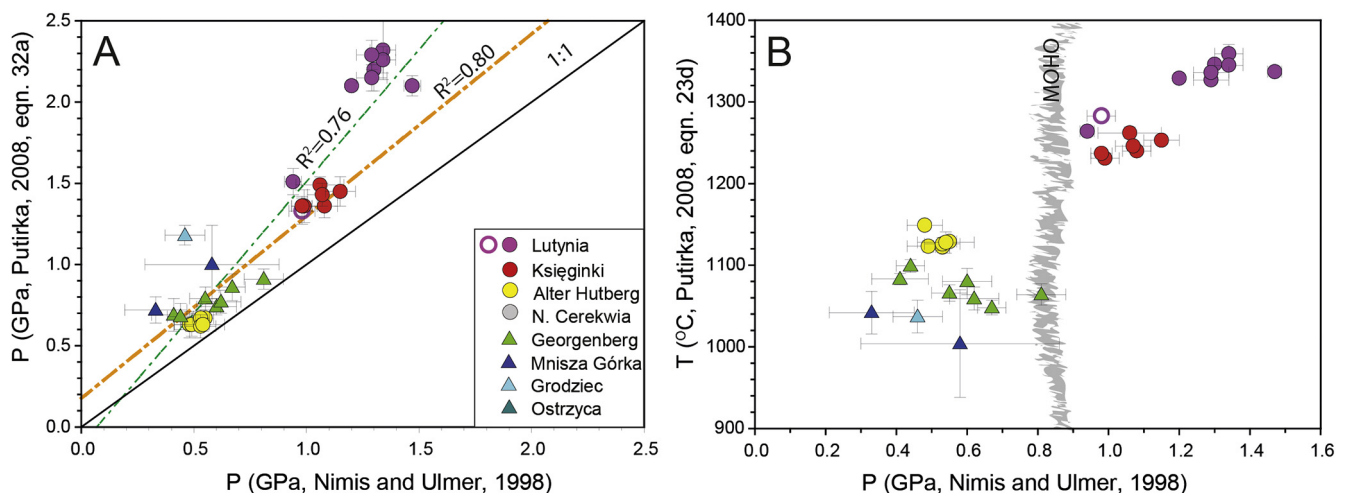


Fig. 7. Thermobarometric estimates of clinopyroxene crystallization. A) comparison of pressures calculated with algorithms by Nimis and Ulmer (1998) and Putirka (2008), eq. 32a) by iteratively applying eq. 32d of Putirka (2008) to obtain a crystallization temperature. The green dashed line is the result of regression of all data, while the orange dashed line illustrates the resulting regression when the data from Lutynia are excluded. The 1:1 correlation line is also shown for comparison. B) P – T conditions for megacryst crystallization along with the approximate pressure of the MOHO. Open circle – the HMg# megacryst.

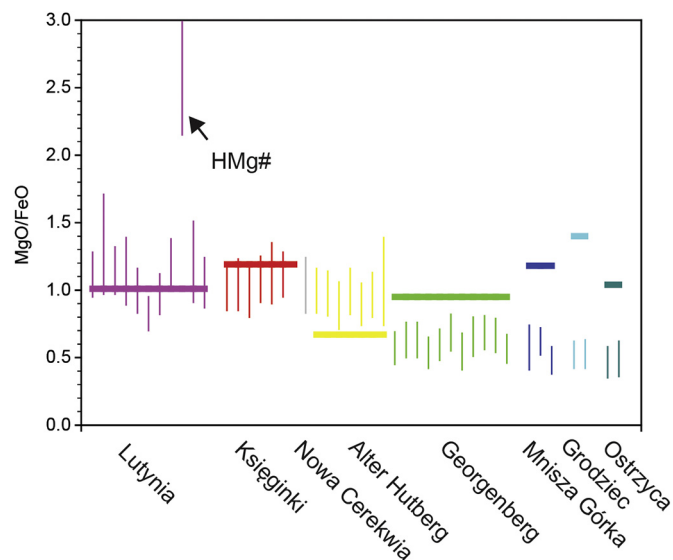


Fig. 8. Comparison of MgO/FeO in theoretical melts in equilibrium with clinopyroxene megacrysts (fine lines) and MgO/FeO from the host lines (bold lines). Partition coefficients after Putirka et al. (1996), composition of host melts from Büchner et al. (2015); Puziewicz et al. (2011), Ladenberger et al., 2004 and author's unpublished data.

megacryst and compared it with composition of DMM and abyssal peridotites. The resulting composition fits well to that of DMM, especially in terms of LREE contents (Fig. 10). Concentrations of some of the more incompatible elements in the homogenized megacryst are lower than in the DMM, which may result from limited (not representative for whole DMM) number of phases in the megacryst. Nevertheless, the presented models allow us to suggest that the HMg# megacryst represents a strongly depleted domain in lithospheric mantle, possibly similar in characteristics to DMM (sensu Workman and Hart, 2005). Isotopic composition of the HMg# megacryst could definitely support this hypothesis, but low concentrations of Sr in spot analyses did not allow to establish reliable isotopic ratios. The lithology represented by the HMg# megacryst possibly experienced slow cooling which allowed unmixing of orthopyroxene from clinopyroxene and their equilibration at relatively low temperatures. According to our knowledge, this is the first description of a clinopyroxene megacryst with DMM characteristics from European Cenozoic volcanic rocks and indeed worldwide.

8.1.2. Origin of medium Mg# megacrysts

The MgO/FeO ratios of hypothetical melts in equilibrium with the MMg# megacrysts vary from 0.70 to 1.71; such values overlap with the MgO/FeO ratios from the host rocks from Księginki and Lutynia (1.19 and 1.01, respectively; Fig. 8), but not that from Alter Hutberg (0.67; Fig. 9). Genetic relationships between the MMg# megacrysts and relatively primary melts from Lutynia and Księginki are suggested also by trace element composition of calculated theoretical melts in equilibrium with the megacrysts (Fig. 9). Those melts resemble the composition of lavas from eastern part of CEVP (formed during low degree melting of primitive mantle source; Ulrych et al., 2011) from which clinopyroxene and minor amounts of olivine are fractionating (Fig. 11, according to modal composition of megacrysts). The fractional crystallization model suggests that megacrysts from Lutynia, Księginki and Nowa Cerekwia formed from the most primitive melts, whereas those from Alter Hutberg formed from more evolved one(s), but not as differentiated as the host tephrite (Fig. 8). Formation of melts in equilibrium with the MMg# megacrysts would require crystallization of up to 80% of the parental melt.

Not all the chemical features of the hypothetical melts in equilibrium with MMg# megacrysts can be explained by fractionation of

clinopyroxene and olivine (e.g. low content of Sr could be explained by crystallization of feldspar; Fig. 11B), but neither geochemical nor modal evidence for presence of additional phase(s) are available (see introduction to section 8.1). In whole model we have used the same clinopyroxene-melt partition coefficients by Hart and Dunn (1993) which were settled for 3 GPa. The high pressure MMg# megacrysts (Lutynia and Księginki) approximately follow the fractionation trends while the low pressure ones (Alter Hutberg) significantly depart from it. This phenomenon may reflect positive correlation between pressure and values of partition coefficients (Green and Pearson, 1983).

Another argument for relationships between MMg# megacrysts (especially those from Księginki and Lutynia) and their host melts are provided by isotopic $^{87}\text{Sr}/^{86}\text{Sr}$ and $^{143}\text{Nd}/^{144}\text{Nd}$ ratios of clinopyroxene, which overlap with those of mafic volcanic rocks from the northern margin of the Bohemian Massif (Fig. 6). Slight variation in $^{87}\text{Sr}/^{86}\text{Sr}$ ratios may result from minor contamination by secondary carbonates, which occur ubiquitously as inclusions in the megacrysts or from contamination of the host melt with crustal material. Alternatively, they could reflect contributions from old metasomatized lithospheric mantle with unradiogenic Nd and radiogenic Sr to their parental magma, but this kind of source for mafic melts in SW Poland was subordinate (Fig. 6; Ladenberger et al., 2004). It is also important to point out that the composition of natural mafic melts from eastern part of CEVP perfectly follows calculated fractionation trends (Fig. 11), which shows that despite megacrysts and the mafic melts have common/similar ancestor, their evolution paths were not identical. All the above discussion indicates that the MMg# megacrysts are in fact antecrysts (sensu Streck, 2008).

One possible source of clinopyroxene megacrysts is the pyroxenitic xenoliths, which are indeed present in some of the Cenozoic volcanic rocks in the studied area (Matusiak-Matek et al., 2017a, 2017b; Puziewicz et al., 2011; Fig. 3). Those are mostly clinopyroxenites and olivine clinopyroxenites interpreted as precipitates from mafic alkaline melts at mantle-depths ($P = 0.86\text{--}1.30$ GPa, $T = 930\text{--}1120$ °C; Op. Cit). Major and trace element compositions of clinopyroxene from those cumulates form up to three (depending on compared elements) compositional fields, but the composition of MMg# megacrysts scarcely overlap with any of them (Fig. 3); it however often follows compositional trends established by data from the cumulates and their trace element composition is strongly similar (Fig. 5C). Moreover, the composition of olivine inclusions ($\text{Fo} = 81.79\text{--}82.19$, $\text{NiO} = 0.08\text{--}0.13$ wt%) in Alter Hutberg and Księginki megacrysts fits well to that of olivine in pyroxenitic cumulates ($\text{Fo} = 77.00\text{--}86.60$, $\text{NiO} = 0.08\text{--}0.30$ wt%, Op. cit). These similarities suggest that MMg# megacrysts may have crystallized from analogous magma as e.g. coarse-grained cumulates in magma conduits (e.g. Robins, 1974). However, one megacryst is probably the result of pyroxenite disintegration as described by (Puziewicz et al. 2011, megacryst 2881; Fig. 3).

8.1.3. Origin of clusters of sulfides

Some of the MMg# clinopyroxene megacrysts from Lutynia and Księginki (and LMg# from Georgenberg) enclose well-defined clusters or streaks formed of rounded inclusions of magnetite and sulfides (Fig. 2B, E). Similar structures, but formed exclusively of sulfides, were described from some of the megacrysts from Massif Central (Woodland and Jugo, 2007), Alaska (Peterson and Francis, 1977), Chukchi Peninsula (Akinin et al., 2005) and others. Peterson and Francis (1977) interpreted this phenomenon as an effect of local oversaturation in sulfur at crystal faces taking place when fast growth of clinopyroxene crystals is not compensated by sulfur diffusion toward the remaining melt. In the studied suite of megacrysts, magnetite inclusions occur together with pyritic ones pointing to their simultaneous crystallization. Coexistence of sulfides and oxides have been described from plutonic and volcanic mafic rocks (e.g. Ciałzela et al., 2018; Keith et al., 2017) and interpreted as a result of oxide crystallization which could trigger

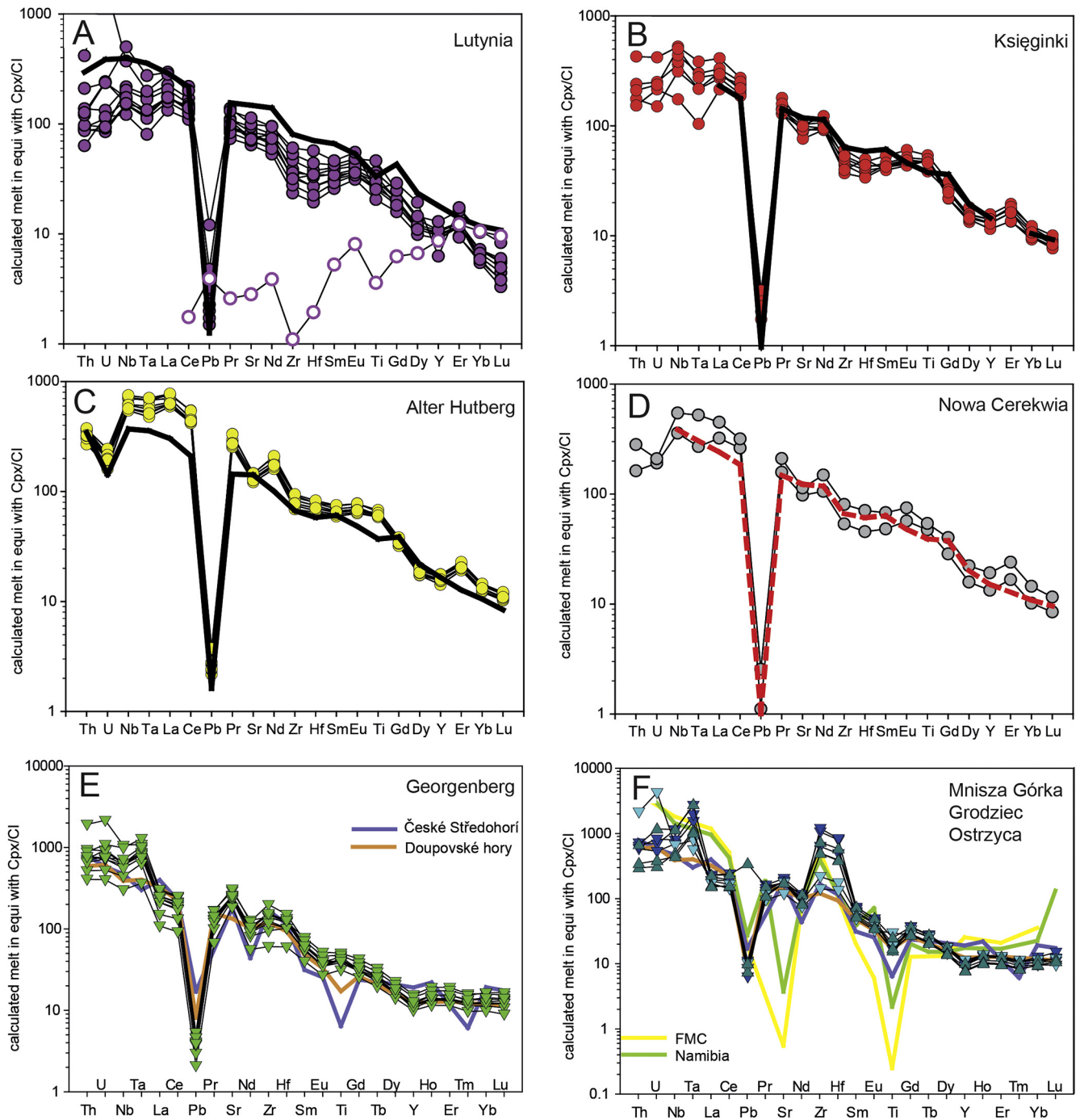


Fig. 9. Calculated melts in equilibrium with clinopyroxene megacrysts compared to composition of natural mafic (A–D; Büchner et al., 2015; Ladenberger et al., 2004 and author's unpublished data) and phonolitic rocks (E–F). The bold lines show composition of host melts (A–D) and selected phonolitic melts E–F (data for: Doupovské hory trachyandesite TV54 after Holub et al. (2010); České Středohoří tinguaita after Ulrich and Balogh, 2000; Namibian phonolite RP-56 after Marsh (2010); French Massif Central phonolite 42,949 after Wilson et al., 1995). Open symbols show the HMg# megacryst. Partition coefficients after Hart and Dunn (1993) for mafic melts and after Mollo et al. (2016) for phonolitic melts, normalization values after McDonough and Sun (1995). Trace element data from host rocks from Nowa Cerekwia (D) are not available and thus were compared to rock from Księginki (red dotted line).

sulfide crystallization by a local decrease of oxygen fugacity. Alternatively, in addition, spinel crystallization could locally decrease the sulfur solubility in the remaining melt, which is strongly dependent on Fe content, the removal of which (with magnetite) would then trigger sulfide crystallization (Wykes et al., 2015). Either way, this observation testifies to rapid growth of MMg# clinopyroxene megacryst, supporting the hypothesis of a magmatic origin, rather than an origin by disaggregation of mantle pyroxenites.

8.1.4. Origin of the low Mg# megacrysts

Clinopyroxene forming LMg# megacrysts record pressures from 0.03 to 1.18 GPa, thus corresponding to lower crust or even MOHO (Puziewicz et al., 2011; Fig. 6). Despite being formed at similar pressures (depths) as the MMg# megacrysts from Nowa Cerekwia and Alter Hutberg, crystallization temperatures are lower (1004–1128 °C).

The LMg# clinopyroxene megacrysts are visually characterized by far more intensive colours (Fig. 2D) than the megacrysts from the

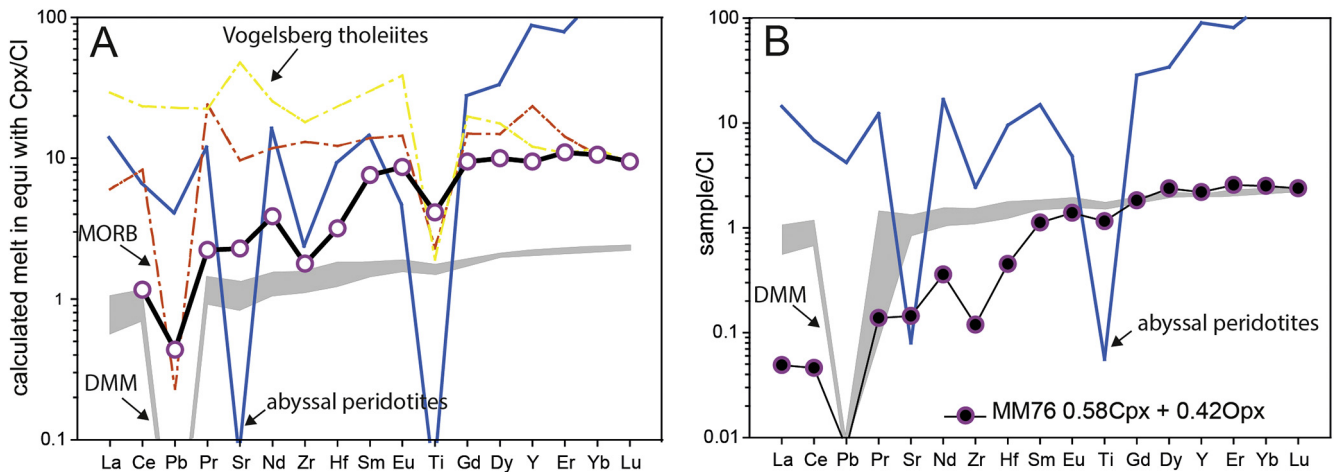


Fig. 10. Composition of melt in equilibrium with HMg# megacryst. A – comparison of compositions of the calculated melt (partition coefficients after Kelemen et al., 2004) with the most depleted tholeiite 2544 from Vogelsberg (Bogaard and Wörner, 2003), the lower range of MORB compositions (Gale et al., 2013), lower range of abyssal peridotites compositions (Niu, 2004) and DMM (Workman and Hart, 2005); B – composition of homogenized HMg# megacryst in comparison to lower range of abyssal peridotites compositions (Niu, 2004) and DMM (Workman and Hart, 2005).

other groups and clinopyroxene from clinopyroxenites. Intensive colouring of megacrysts and porphyrocrysts of Na and Fe-rich and Cr-poor clinopyroxene had been interpreted as: 1) a manifestation of their origin from evolved melts; 2) a feature inherited from pyroxenites or 3) granulites whose disintegration released single clinopyroxene crystals (e.g. Dobosi, 1989; Duda and Schmincke, 1985; Jankovics et al., 2016; Shaw and Eyzaguirre, 2000). A metamorphic origin can be excluded, as this group of megacrysts enclose type II (O'Reilly and Griffin, 2000; Fig. 4), typically magmatic apatite. Moreover, granulitic xenoliths have not been described from the study area.

8.1.4.1. Low Mg# megacrysts from Georgenberg. Megacrysts from Georgenberg differ from other LMg# megacrysts by their higher Al_2O_3 and lower CaO and Na_2O contents (Fig. 3) and thus origin of the two subgroups of megacrysts is discussed separately. Hypothetical melts in equilibrium with Georgenberg megacrysts have MgO/FeO ratios of 0.42–0.82, which are different from that of the host nephelinite (0.95). This suggests that the megacrysts must have originated from a more Fe-rich magma than their host, which is also evidenced by low Ni content in sulfide inclusions in the clinopyroxene (Ciążela et al., 2018 and references therein, Electronic Table A9). Lack of equilibrium between megacrysts and host melt is mirrored also in the presence of newly crystallized rims (Table 1).

Clinopyroxene megacrysts rich in FeO and Al_2O_3 similar to those from Georgenberg were reported from the Pannonian Basin by (Dobosi and Jenner, 1999; Fig. 3) and interpreted as precipitates from fractionated alkali mafic melt. More recently, Loges et al. (2019) suggested that similar green-core clinopyroxene are products of crystallization of strongly alkaline, Fe-rich melts (tephriphonolite). Clinopyroxene from Georgenberg contains apatite inclusions, is rich in Al and the Na contents are similar to those reported from the Pannonian Basin (Fig. 3). Thus it is plausible that the Georgenberg megacrysts formed from an evolved alkaline melt. Indeed, the calculated composition of melt in equilibrium with the Georgenberg megacrysts resembles that of phonolite from Doupské hory (Holub et al., 2010) and České Středohoří Volcanic Complexes (Ulrych and Balogh, 2000; Fig. 8), both occurring in the axis of the Eger Graben (Fig. 1). Therefore megacrysts from Georgenberg seem to be cognate with phonolite/tephriphonolite-like melt and variations in composition of the Georgenberg megacrysts may be explained by crystallization at depth from differentiated strongly alkaline melt (Fig. 11C). Fine-grained structures present occurring together with the Georgenberg megacrysts (Fig. 2) were interpreted by Shaw

(2009) as products of amphibole breakdown at crustal pressures. The presence of those relicts point to the parental melt having been hydrous. The presence of apatite also requires a hydrous melt, as well as saturation in phosphorous, while the occurrence of titanomagnetite implies high contents of Ti and Fe (Fig. 11).

8.1.4.2. Low Mg# megacrysts from Grodziec, Ostrzyca and Mnisza Górka. The megacrysts from Grodziec, Mnisza Górka and Ostrzyca (GMO) are characterized by very intensive colouring (Fig. 2), which may have variable origins, as discussed above. Pyroxenitic xenoliths from the three localities are scarce, and those that have been studied have different textural and chemical characteristics (Fig. 3; Matusiak-Matek et al., 2017b and author's unpublished data) than the megacrysts. Thus, an origin of LMg# clinopyroxene as fragments of disintegrated pyroxenites can be excluded. Lipa et al. (2014) demonstrated that the megacrysts from Ostrzyca formed from fractionated FeO-rich basanite. This interpretation is similar to that of type III megacrysts from the west Eifel (Shaw and Eyzaguirre, 2000; Fig. 3), which are precipitates from FeO-rich melts under upper-mantle conditions. Also, Loges et al. (2019) suggested a phonolite-related origin of green clinopyroxene porphyrocrysts occurring in basanite from western shoulder of Eger Graben.

Therefore, we have calculated the trace element composition of alkaline melts in equilibrium with GMO LMg# megacrysts. The hypothetical melts for Grodziec megacrysts fit quite well to the composition of phonolite-like melts from the Eger Graben, differing in having higher Th, U and Ta contents. The melt in equilibrium with megacrysts from Ostrzyca and Mnisza Górka, despite a general resemblance to the reference melts (and melt in equilibrium with megacrysts from Georgenberg), are significantly richer in Ta, Zr and Hf (Fig. 8). Nevertheless, if a common parental melt for GMO megacrysts is assumed (lack of apatite in samples from Mnisza Górka and Grodziec may be only a sampling artefact), it would be a hydrous and P-saturated melt capable of producing significant amounts of hydroxyapatite. The LMg# megacrysts formed from melts being isotopically related to their host melt and thus are of antecrystic nature.

All the calculated melts show strong enrichment in Ta, but not in Nb. Decoupling of Ta from Nb can be explained by kinematic fractionation during crystallization of Ti-oxides (Marschall et al., 2013) or by their crystallization in a range of oxygen fugacities where Nb is compatible and Ta is incompatible (Cartier et al., 2014); presence of Ti-oxides have however not been stated in paragenesis with clinopyroxene. The positive anomalies in Zr and Hf contents in the GMO megacrysts are

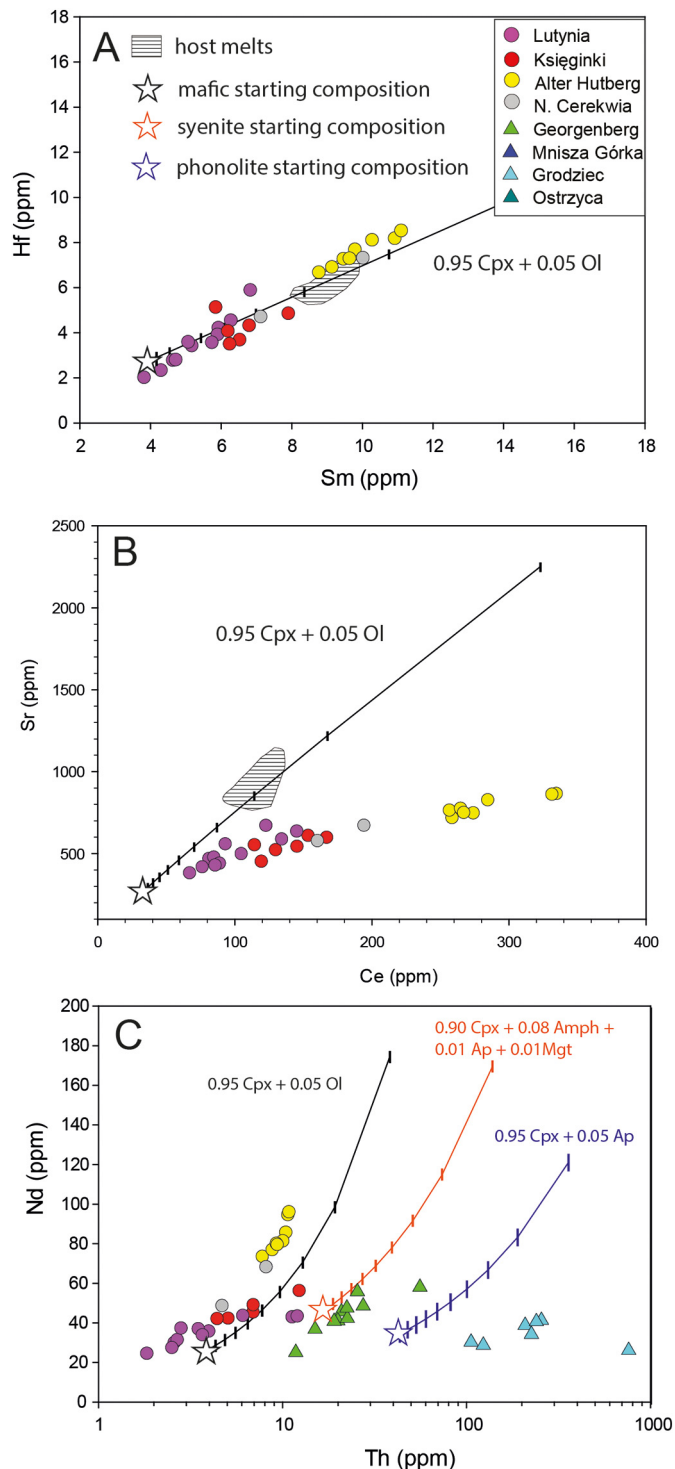


Fig. 11. Composition of melts in equilibrium with clinopyroxene megacrysts compared to differentiations trends of mafic (A, B, C) and phonolitic melts (C). A) Differentiation trends of melt derived from melting of primitive mantle (starting composition = 0.5% dynamic melting in garnet facies conditions followed by 1.5% of melting in spinel facies conditions); B) Ce–Sr differentiation trend of a “mafic starting composition” melt; C) Th–Nd differentiations trends for (from left to right): 1) mafic melt of a “starting composition” as in A and B; 2) sodalite monzosyenite TV-54 from Doupské hory Volcanic Complex (Holub et al., 2010); the most fractionated phonolite from 3) Doupské hory Volcanic Complex (Holub et al., 2010). Notations in the diagrams point modal proportions of crystallizing phases. Vertical lines at trendlines show the amount of remaining melt, crystallization ends at 10% of melt in the system. The calculations employed the Petromodeler spreadsheet (Ersoy, 2013), partition coefficients after Mollo et al. (2016), Hart and Dunn (1993), Green and Pearson, 1983, and Larsen (1979).

not typical for megacrystic clinopyroxene. This feature could be simply explained by of the sample contamination by inclusions, but: 1) careful examination of BSE images did not indicated the presence of any inclusions; 2) time-resolved trace element patterns for those elements are smooth and do not show any abrupt increase in Zr and Hf contents. The positive Zr–Hf anomalies may result also from the composition of the host melts (e.g. their contamination by slab-derived hydrous fluids (Coltorti et al., 2007) or the presence of dissolve zircon (e.g. Siebel et al., 2009). However, all the LMg# megacrysts are products of crystallization from strongly fractionated alkaline melts, where positive Zr–Hf anomalies in clinopyroxene are common and reflects the strongly enhanced partitioning of these elements into Na-rich varieties of clinopyroxene (e.g. Batki et al., 2018; Marks et al., 2004). Thus, positive Zr–Hf anomalies in megacrysts seem to be natural consequence of the nature of the parental melt(s).

The theoretical melt in equilibrium with Ostrzyca and Mnisza Górka megacrysts is enriched in Zr and Hf, but the absolute contents (Zr: 480–1170 ppm; Hf: 370–810 ppm) are different than those from alkaline rocks from Eger Graben (Zr: 201–656 ppm; Hf: ~6.00–2.00 ppm; Holub et al., 2010; Ulrych and Balogh, 2000) and reach the values close to those from very strongly evolved alkaline melts (maximum Zr values from Namibian and French phonolite-like melts are 1500 and 2090 ppm, respectively; Marsh, 2010; Wilson et al., 1995), while Zr–Hf content in clinopyroxene resembles that from clinopyroxene occurring in alkaline intrusions in Greenland and Kola Peninsula (e.g. Arzamastsev et al., 2005; Marks et al., 2004). This similarity suggests that the megacrysts enriched in Zr and Hf could have formed from very strongly fractionated alkaline melts. Those melts would however needed to be selectively enriched in elements like Zr, Hf, Sr and Sm, as content of other elements mimic that in megacrysts from Georgenberg.

8.2. Relations between megacrysts' parental melts

The megacrysts from Księginki, Lutynia (both MMg#) and Ostrzyca (LMg#) have similar isotopic composition (Fig. 6). As chemical data from those three localities always delineates the “boundary” compositions (e.g. Figs. 3, 4), we assume that their isotopic compositions also represents the range for the entire megacryst suite. This assumption further implies that all megacrysts crystallized from melts originating from a similar source, but at variable stages of differentiation.

As previously discussed, the MMg# megacrysts possibly crystallized from fractionating mafic melt formed by melting in the upper mantle; fractionation of the same melts resulted in formation of mafic volcanic rocks in the study area (Fig. 11). The LMg# megacrysts from Georgenberg were formed from significantly less mafic alkaline melts, but their major and trace element composition (Fig. 3) and fractionation trends (Fig. 11) are always parallel to those from MMg# megacrysts pointing possible genetic affinities between parental melts for the two groups.

The relation of melts parental for the GMO megacrysts and those parental for other megacrysts is far more complicated. The first example comes from Al_2O_3 and TiO_2 contents which are lower than in Georgenberg megacrysts (Fig. 3). This inconsistency may result either from different parental melts or change in chemophysical conditions of crystallization (e.g. temperature decrease; Fig. 6) or, possibly, both. Furthermore, the composition of melts in equilibrium with the GMO megacrysts cannot be compared to those from natural alkaline melts, even those with extreme composition (Fig. 10). The untypical trace element composition of the GMO megacrysts, the inability to model an origin of their parental melt(s) (despite we know it is somehow related to Cenozoic volcanism) and equivocal estimations of the physical conditions of their formation (Electronic table A3) suggest that only detailed reconstruction of the mineral composition of the source rocks for the GMO megacrysts will allow full understanding of their origin.

9. Conclusions: Megacrysts in mafic lavas as messengers from mantle and crust

The majority of the clinopyroxene megacrysts from the northern margin of the Bohemian Massif are precipitates from variable differentiates of mafic melts and thus carry a vast amount of information about the evolution of host melts from mantle depths to the crust. This information is inaccessible from either xenoliths or from studying the host basaltic melts themselves.

Almost all of the studied megacrysts follow the fractionation trend of melts derived from melting of primitive mantle. The first precipitates from the mafic melt are known mostly from clinopyroxenitic xenoliths (Fig. 3), whereas megacrysts that formed from such primitive melts are scarce (megacryst 2881 from Księginki; Puziewicz et al., 2011). Precipitation of clinopyroxene from slightly more evolved melts resulted in formation of MMg# megacrysts. Within this group, a fractionation trend is observable: 1) megacrysts from Lutynia and Księginki formed at mantle depths from MgO-rich, locally sulfur-saturated melts (presence of inclusions of sulfides); 2) megacrysts from Alter Hutberg and Nowa Cerekwia also formed from mafic, but more fractionated melts at lower/middle crustal pressures (Figs. 7, 8 and 11). The LMg# megacrysts formed at lower/middle-crustal conditions from the most evolved, phonolite-like melts related to Cenozoic magmatic activity. The compositional details of the melts parental to the LMg# megacrysts are, however, different in Lusatia and Lower Silesia. The presented data led us to conclude that almost all of the megacrysts come from syn-volcanic coarse-grained bodies/veins formed in magma batches temporarily residing at uppermost mantle and low/mid crustal depths. Although all the precipitative megacrysts are cognate with mafic melts, we have shown that numerous scenarios of megacrysts formation are possible, even at a geographically relatively small area.

The proposed scheme of evolution of alkaline melts follows that presented by Woodland and Jugo (2007) for megacrysts from the Devès volcanic field (French Massif Central). However, in their study, megacrysts representing different stages of evolution of a melt occur together in two outcrops located close to each other (~20 km), while in SE Germany and SW Poland in a single outcrop megacrysts formed during only one stage of melt evolution are typically present. Therefore, we suggest that megacrysts formed in separated bodies (e.g. magma conduits) located at variable depths, to which batches of variably evolved melts were delivered – the shallower the magmatic body was emplaced, the more evolved melt was delivered to it. In general, no correlation occurs between the spatial distribution of outcrops, their age and the stage of evolution of melts from which the megacrysts formed; the only exceptions are the GMO LMg# megacrysts which occur in the vicinity of Złotoryja (Fig. 1). Those megacrysts could have formed within single crustal intrusion, but no geophysical data implying the presence of such a big (~18 km long) igneous body is available for this area (Petecki and Rosowiecka, 2017). The GMO and Georgenberg LMg# megacrysts are evidences for strongly alkaline, intermediate volcanism. Manifestations of this kinds of volcanic activity are common in the Czech and E German part of CEVP, but, to our best knowledge, it was not previously described from Polish part of the province.

The HMg# megacryst described here does not follow the fractionation trend of mafic magma. This megacryst represents part of coarse-grained rock occurring in the DMM-like mantle. According to our knowledge, this is the first description of a clinopyroxene megacryst of this kind in Europe and worldwide.

Variations in chemical composition of the studied clinopyroxene megacrysts resulting from origins at varying conditions and from varying host melts show that megacrysts should be considered as an important, but not straightforward, source of information about the evolution of mantle-derived melts and the plumbing of magmatic systems (even those which did not reach the surface) and may carry information about their mantle source rocks.

Declaration of Competing Interest

The authors declare that they have no known competing financial interests or personal relationships that could have appeared to influence the work reported in this paper.

Acknowledgements

We are deeply grateful to Szabolcs Harangi and an anonymous reviewer for valuable comments and to editor Greg Shellnutt for help with manuscript handling. Jana Ďurišová from Czech Academy of Sciences is thanked for help in LA ICP-MS analyses and Lidia Ježak for microprobe work. Michał Dajek and Danuta Lipa are thanked for preparation of maps, Danuta is thanked also for help in analytical work. Jakub Ciążela is thanked for help with sulfides data handling and Anna Pietranik is thanked for discussions. This study was possible thanks to the project no. UMO-2014/15/B/ST10/00095 of Polish National Centre for Science for JP, and to the bilateral Austrian-Polish projects (WTZ PL 08/2018, WTZ PL16). FIERCE is financially supported by the Wilhelm and Else Heraeus Foundation and by the Deutsche Forschungsgemeinschaft (DFG, INST 161/921-1 FUGG and INST 161/923-1 FUGG), which is gratefully acknowledged. This is FIERCE contribution No. 53. Publication of this article in open access was financially supported by the Excellence Initiative – Research University (IDUB) programme for the University of Wrocław

Appendix A. Supplementary data

Supplementary data to this article can be found online at <https://doi.org/10.1016/j.lithos.2020.105936>.

References

- Ackerman, L., Špaček, P., Medaris Jr., G., Hegner, E., Svojtka, M., Ulrych, J., 2012. Geochemistry and petrology of pyroxenite xenoliths from Cenozoic alkaline lava, Bohemian Massif. *J. Geosci.* 58, 199–219.
- Akinin, V.V., Sobolev, A., Ntaflou, T., Richter, W., 2005. Clinopyroxene megacrysts from Enmelen melanephelinitic volcanoes (Chukchi Peninsula, Russia): application to composition and evolution of mantle melts. *Contrib. Mineral. Petrol.* 150, 85–101.
- Arzamastsev, A., Bea, F., Arzamastseva, L.V., Montero, P., 2005. Trace elements in minerals of the Khibiny Massif as indicators of mineral formation evolution: results of LA-ICP-MS study. *Geochem. Int.* 43, 71–85.
- Ashchepkov, I.V., André, L., Downes, H., Belyatsky, B.A., 2011. Pyroxenites and megacrysts from Vitim picrite-basalts (Russia): Polybaric fractionation of rising melts in the mantle? *J. Asian Earth Sci.* 42, 14–37.
- Badura, J., Pécskay, Z., Koszowska, E., Wolska, A., Zuchiewicz, W., Przybylski, B., 2006. New data on age and petrological properties of lower Silesian Cenozoic basaltoids, SW Poland. *Prz. Geol.* 54, 145–153.
- Batki, A., Pál-Molnár Jankovics, É., Kerr, A.C., Kiss, B., Markl, G., Heincz, A., Harangi, S., 2018. Insights into the evolution of an alkaline magmatic system: an in situ trace element study of clinopyroxenes from the Ditrău Alkaline Massif, Romania. *Lithos* 300–301, 51–71.
- Birkenmajer, K., Pécskay, Z., 2002. Radiometric dating of the Tertiary volcanics in lower Silesia, Poland. I. Alkali basaltic rocks of the Opole region. *Bull. Polish Acad. Sci. Earth Sci.* 50, 31–50.
- Birkenmajer, K., Pécskay, Z., Grabowski, J., Lorenc, M.W., Zagożdżon, P., 2011. Radiometric dating of the Tertiary volcanics in lower Silesia, Poland. VIK-Ar and paleomagnetic data from basaltic rocks of the West Sudety mountains and their northern foreland. *Ann. Soc. Geol. Pol.* 81, 115–131.
- Blusztajn, J., Hart, R.S., 1989. Sr, Nd and Pb isotopic character of Tertiary basalts from Southwest Poland. *Geochim. Cosmochim. Acta* 53, 2689–2696.
- Bogaard, P.J.F., Wörner, G., 2003. Petrogenesis of Basaltic to Tholeiitic Volcanic Rocks from the Miocene Vogelsberg, Central Germany. *J. Petrol.* 44, 569–602.
- Brey, G.P., Köhler, T., 1990. Geothermobarometry in four-phase lherzolites II. New thermobarometers and practical assessment of existing thermobarometers. *J. Petrol.* 31, 1353–1378.
- Büchner, J., Tietz, O., Viereck, L., Suhr, P., Abratis, M., 2015. Volcanology, geochemistry and age of the Lausitz Volcanic Field. *Int. J. Earth Sci.* 104, 2057–2083.
- Bussweiler, Y., Pearson, G.D., Stachel, T., Kjarsgaard, B.A., 2018. Cr-rich megacrysts of clinopyroxene and garnet from Lac de Gras kimberlites, Slave Craton, Canada – implications for the origin of clinopyroxene and garnet in cratonic lherzolites. *Mineral. Petrol.* 112 (Suppl 2), S583–S596.
- Canil, D., O'Neill, H.S., 1996. Distribution of ferric iron in some upper mantle assemblages. *J. Petrol.* 37, 609–635.

- Cartier, C., Hammouada, T., Boyet, M., Bouhifd, M.A., Devidal, J.-L., 2014. Redox control of the fractionation of niobium and tantalum during planetary accretion and core formation. *Nat. Geosci.* 7 (8), 573–576.
- Ciążela, J., Koepke, J., Dick, H. J. B., Botcharnikov, R., Muszyński, A., Lazarov, M., Schuth, S., Pieterek, B., Kuhn, T., 2018. Sulfide at an oceanic crust-mantle transition zone: Kane Megamullion (23°N, MAR). *Geochim. Cosmochim. Acta* 230, 155–189.
- Coltorti, M., Bonadiman, C., Faccini, B., Ntaflou, T., Siena, F., 2007. Slab melt and intraplate metasomatism in Kapfenstein mantle xenoliths (Styrian Basin, Austria). *Lithos* 94, 66–89.
- Dawson, J.B., 1980. *Kimberlites and their Xenoliths*. Springer Verlag, New York.
- Dèzes, P., Schmid, S.M., Ziegler, P.A., 2004. Evolution of the European Cenozoic Rift Systems: Interaction of the Alpine and Pyrenean orogens with their foreland lithosphere. *Tectonophysics* 389, 1–33.
- Dobosi, G., 1989. Clinopyroxene zoning patterns in the young alkali basalts of Hungary and their petrogenetic significance. *Contrib. Mineral. Petrol.* 101, 112–121.
- Dobosi, G., Jenner, G.A., 1999. Petrologic implications of trace element variation in clinopyroxene megacrysts from the Nógrád volcanic province, North Hungary: a study by laser ablation microprobe-inductively coupled plasma-mass spectrometry. *Lithos* 46, 731–749.
- Dobosi, G., Downes, H., Embey-Isztin, A., Jenner, G.A., 2003. Origin of megacrysts and pyroxenite xenoliths from the Pliocene alkali basalts of the Pannonian Basin (Hungary). *Neues Jahrbuch für Mineralogie - Abhandlungen* 178, 217–237.
- Duda, A., Schmincke, H.-U., 1985. Polybaric differentiation of alkali basaltic magmas: evidence from green-core clinopyroxenes (Eifel, FRG). *Contrib. Mineral. Petrol.* 91, 340–353.
- Ersoy, E.Y., 2013. *PETROMODELER (Petrological Modeler): a Microsoft Excel® spreadsheet program for modelling melting, mixing, crystallization and assimilation processes in magmatic systems*. *Turk. J. Earth Sci.* 22, 115–125.
- Gale, A., Dalton, C.A., Langmuir, C.H., Su, Y., Shilling, J.-G., 2013. The mean composition of ocean ridge basalts. *Geochim. Geophys. Geosyst.* 14, 489–518.
- Gernon, T.M., Upton, B.G.J., Ugra, R., Yücel, C., Taylor, R.N., Elliott, H., 2016. Complex subvolcanic magma plumbing system of an alkali basaltic maar-diatreme volcano (Elie Ness, Fife, Scotland). *Lithos* 264, 70–85.
- Green, T.H., Pearson, N.J., 1983. Effect of pressure on rare earth element partition coefficients in common magmas. *Nature* 305, 414–416.
- Hammer, J., Jacob, S., Welsch, B., Hellebrand, E., Sinton, J., 2016. Clinopyroxene in postshield Haleakala ankaramite: 1. Efficacy of thermobarometry. *Contrib. Mineral. Petrol.* 171, 1.
- Hart, S.R., Dunn, T., 1993. Experimental cpx/melt partitioning of 24 trace elements. *Contrib. Mineral. Petrol.* 113, 1–8.
- He, D., Liu, Y., Tong, X., Zong, K., Hu, Z., Gao, S., 2013. Multiple exsolutions in a rare clinopyroxene megacrysts from the Hannuoba basalt, North China: Implications for subducted slab-related crustal thickening and recycling. *Lithos* 177, 136–147.
- Holub, F.V., Rappich, V., Erban, V., Pécskay, Z., Mlčoch, B., Míková, J., 2010. Petrology and geochemistry of the Tertiary alkaline intrusive rocks at Doupov, Doupovské hory Volcanic complex (NW Bohemian Massif). *J. Geosci.* 55, 251–278.
- Jankovics, É., Tarasćák, Z., Dobosi, G., Embey-Isztin, A., Batki, A., Harangi, S., Hauzenberger, C., 2016. Clinopyroxene with diverse origin in alkali basalts from the western Pannonian Basin: Implications from trace element characteristics. *Lithos* 262, 120–134.
- Kargin, A.V., Sazonova, L.V., Nosova, A.A., Lebedeva, N.M., Tretyachenko, V.V., Abersteiner, A., 2017. Cr-rich clinopyroxene megacrysts from the Grib kimberlite, Arkhangelsk province, Russia: Relation to clinopyroxene-phlogopite xenoliths and evidence for mantle metasomatism by kimberlite melt. *Lithos* 292–293, 34–38.
- Keith, M., Hasse, K.M., Klemd, R., Schwarz-Schampera, U., Franke, H., 2017. Systematic variations in magmatic sulphide chemistry from mid-ocean ridges, back-arc basins and island arcs. *Chem. Geol.* 451, 67–77.
- Kelemen, P.B., Yagodinski, G.M., Scholl, D.W., 2004. Along-strike variation in lavas of the Aleutian Island Arc: Implications for the genesis of high Mg# andesite and the continental crust. In: Eiler, J. (Ed.), *AGU Geophysical Monograph Series*. 138, pp. 223–276.
- Kopylova, M.G., Nowell, G.M., Pearson, D.G., Markov, G., 2009. Crystallization of megacrysts from protokimberlitic fluids: Geochemical evidence for high-Cr megacrysts in the Jericho kimberlite. *Lithos* 112S, 284–295.
- Kostrovitsky, S.I., Malkovets, V.G., Verichev, E.M., Garaniin, V.K., Suvorova, L.V., 2004. Megacrysts from the Grib kimberlite pipe (Arkhangelsk Province, Russia). *Lithos* 77, 511–523.
- Kozłowska Koch, M., 1981. Petrography of Ultramafic Nodules in the Nephelinites from Księginki near Lubań (Lower Silesia) (Archiwum Mineralogiczne XXXVII).
- Kukuła, A., Puziewicz, J., Matusiak-Małek, M., Ntaflou, T., Büchner, J., Tietz, O., 2015. Depleted subcontinental lithospheric mantle and its tholeiitic melt metasomatism beneath NE termination of the Eger Rift (Europe): the case study of the Steinberg (Upper Lusatia, SE Germany) xenoliths. *Mineral. Petrol.* 109, 761–787.
- Ladenberger, A., Peate, D.W., Baker, J.A., Michalik, M., 2004. Pb-Hf-Nd isotope compositions of Tertiary lower Silesia basalts (SW Poland). *Geochim. Cosmochim. Acta* 68, A725.
- Larsen, L.M., 1979. Distribution of REE and Other Trace-elements between Phenocrysts and Peralkaline Undersaturated Magmas, Exemplified by Rocks from the Gardar Igneous Province, South Greenland. *Lithos* 12, 303–315.
- Liang, Y., Sun, C., Yao, L., 2013. A REE-in-two-pyroxene thermometer for mafic and ultramafic rocks. *Geochim. Cosmochim. Acta* 102, 246–260.
- Lipa, D., Puziewicz, J., Ntaflou, T., Matusiak-Małek, M., 2014. Clinopyroxene megacrysts from basanite from Ostrzyca Proboszczowicka in Lower Silesia (SW Poland). *Geosci. Notes* 2, 49–72.
- Liu, Y.-D., Ying, J.-F., 2019. Origin of clinopyroxene megacrysts in volcanic rocks from the North China Craton: a comparison study with megacrysts worldwide. *Int. Geol. Rev.* <https://doi.org/10.1080/00206814.2019.1663766>.
- Loges, A., Schultze, D., Klügel, A., Lucassen, F., 2019. Phonolitic melt production by carbonatite Mantle metasomatism: evidence from Eger Graben xenoliths. *Contrib. Mineral. Petrol.* 174, 93.
- Majdański, M., Grad, M., Guterch, A., SUDETES 2003 Working Group, 2006. 2-D seismic tomographic and ray tracing modelling of the crustal structure across the Sudetes Mountains basing on SUDETES 2003 experiment data. *Tectonophysics* 412, 249–269.
- Marks, M., Halama, R., Wenzel, T., Markl, G., 2004. Trace element variations in clinopyroxene and amphibole from alkaline to peralkaline syenites and granites: implications for mineral-melt trace-element partitioning. *Chem. Geol.* 211, 185–215.
- Marschall, H.R., Dohmes, R., Ludwig, T., 2013. Diffusion-induced fractionation of niobium and tantalum during continental crust formation. *Earth Planet. Sci. Lett.* 375, 361–371.
- Marsh, J., 2010. The geochemistry and evolution of Palaeogene phonolites, Central Namibia. *Lithos* 117, 149–160.
- Matusiak-Małek, M., Puziewicz, J., Ntaflou, T., Grégoire, M., Downes, H., 2010. Metasomatic effects in the lithospheric mantle beneath the NE Bohemian Massif: A case study of Lutynia (SW Poland) peridotite xenoliths. *Lithos* 117, 49–60.
- Matusiak-Małek, M., Puziewicz, J., Ntaflou, T., Grégoire, M., Kukuła, A., Wojtulek, P.M., 2017a. Origin and evolution of rare amphibole-bearing peridotites from Wilcza Góra (SW Poland), Central Europe. *Lithos* 286–284, 302–323.
- Matusiak-Małek, M., Cwiek, M., Puziewicz, J., Ntaflou, T., 2017b. Thermal and metasomatic rejuvenation and dunitization in lithospheric mantle beneath Central Europe - the Grodziec (SW Poland) case study. *Lithos* 276, 15–29.
- McDonough, W.F., Sun, S.S., 1995. The composition of the Earth. *Chem. Geol.* 120, 223–253.
- Mollo, S., Blundy, J., Iezzi, G., Scarlato, P., 2013. The partitioning of trace elements between clinopyroxene and trachybasaltic melt during rapid cooling and crystal growth. *Contrib. Mineral. Petrol.* 166, 1633–1654.
- Mollo, S., Forni, F., Bachmann, O., Blundy, J.D., De Astis, G., Scarlato, P., 2016. Trace element partitioning between clinopyroxene and trachy-clinopyroxene melts: A case study from the Campanian Ignimbrite (Campi Flegrei, Italy). *Lithos* 252–253, 160–172.
- Morimoto, N., 1989. Nomenclature of pyroxenes. Submission of new minerals and mineral names. *International mineralogical association. Can. Mineral.* 27, 143–156.
- Müller, W., Shelley, M., Miler, P., Broude, S., 2009. Initial performance metrics on a new custom-designed ArF excimer LA-ICPMS system coupled to a two-volume laser-ablation cell. *J. Anal. At. Spectrom.* 24, 209–214.
- Nimis, P., Taylor, W.R., 2000. Single clinopyroxene thermobarometry for garnet peridotites. Part 1. Calibration and testing of a Cr-in-cpx barometer and an enstatite-in-cpx thermometer. *Contrib. Mineral. Petrol.* 139, 541–554.
- Nimis, P., Ulmer, P., 1998. Clinopyroxene geobarometry of magmatic rocks. Part 1: an expanded structural geobarometer for anhydrous and hydrous, basic and ultrabasic systems. *Contrib. Mineral. Petrol.* 133, 122–135.
- Niu, Y., 2004. Bulk-rock major and trace element compositions of abyssal peridotites: implications for mantle melting, melt extraction and post-melting processes beneath mid-ocean ridges. *J. Petrol.* 45, 2426–2458.
- Ntaflou, T., Puziewicz, J., Matusiak-Małek, M., 2013. Insight into Cenozoic alkaline basalts from SW Poland: high mantle potential temperatures as an evidence for local thermal anomalies ("finger plume"). *Basalt 2013. Cenozoic Magmatism in Central Europe*. Görlitz, Germany, pp. 24–25.
- O'Reilly, S.Y., Griffin, W.L., 2000. Apatite in the mantle: implications for metasomatic processes and high heat production in Phanerozoic mantle. *Lithos* 53, 217–232.
- Patifio Douce, A.E., Roden, M.F., Chaumba, J.B., Fleisher, C., Yagodinski, G., 2011. Compositional variability of terrestrial mantle apatites, thermodynamic modelling of apatite volatile contents, and the halogen and water budgets of planetary mantles. *Chem. Geol.* 288, 14–31.
- Pécskay, Z., Birkenmajer, K., 2013. Insight into the geochronology of Cenozoic alkaline basaltic volcanic activity in Lower Silesia (SW Poland) and adjacent areas. *Basalt 2013. Cenozoic Magmatism in Central Europe*. Görlitz, Germany, pp. 66–67.
- Petecki, Z., Rosowiecka, O., 2017. A new magnetic anomaly map of Poland and its contribution to the recognition of crystalline basement rocks. *Geol. Quart.* 61, 934–945.
- Peterson, R., Francis, D., 1977. The origin of sulfide inclusions in pyroxene megacrysts. *Am. Mineral.* 62, 1049–1051.
- Pivin, M., Fémenias, O., Demaiffe, D., 2009. Metasomatic mantle origin for Mbuji-Mayi and Kundelungu garnet and clinopyroxene megacrysts (Democratic Republic of Congo). *Lithos* 112, 951–960.
- Putirka, K.D., 2008. Thermometers and barometers for volcanic systems. *Minerals, Inclusions and Volcanic Processes*. In: Putirka, K.D., Tepley III, F.J. (Eds.), *Reviews in mineralogy and geochemistry*. Mineralogical Society of America, Geochemical Society.
- Putirka, K., Johnson, M., Kinzler, R., Longhi, J., Walker, D., 1996. Thermobarometry of mafic igneous rocks based on clinopyroxene-liquid equilibria, 0–30 kbar. *Contrib. Mineral. Petrol.* 123, 92–108.
- Puziewicz, J., Koepke, J., Grégoire, M., Ntaflou, T., Matusiak-Małek, M., 2011. Lithospheric Mantle Modification during Cenozoic Rifting in Central Europe: evidence from the Księginki nephelinite (SW Poland) xenolith suite. *J. Petrol.* 53, 2107–2145.
- Puziewicz, J., Matusiak-Małek, M., Ntaflou, T., Grégoire, M., Kukuła, A., 2015. Subcontinental lithospheric mantle beneath Central Europe. *Int. J. Earth Sci.* 104, 1913–1924.
- Rankenburg, K., Lassiter, J.C., Brey, G., 2004. Origin of megacrysts in volcanic rocks of the Cameroon volcanic chain- constraints on magma genesis and crustal contamination. *Contrib. Mineral. Petrol.* 147, 129–144.
- Righter, K., Carmichael, I.S.E., 1993. Mega-xenocrysts in alkali olivine basalts: Fragments of disrupted mantle assemblages. *Am. Mineral.* 78, 1230–1245.
- Roberts, R.J., Lehong, K.D., Botha, A.E.J., Costin, G., De Beer, F.C., Hoffman, W.J., Hetherington, C.J., 2019. Clinopyroxene megacrysts from Marion Island, Antarctic Ocean: evidence for a late stage shallow origin. *Mineral. Petrol.* 113, 155–167.
- Robins, B., 1974. Synorogenic alkaline pyroxenite dykes on Seiland, Northern Norway. *Nor. Geol. Tidsskr.* 54, 247–268.

- Roduit, N., 2007. JMicroVision : un Logiciel D'analyse D'images Pétrographiques Polyvalent. PhD Thesis. Université de Genève (in French).
- Sawicki, L., 1995. Geological Map of Lower Silesia with Adjacent Czech and German Territories (without Quaternary Deposits). Polish Geological Institute, Warszawa.
- Schmidt, M.E., Schrader, C.M., Crumpler, L.S., Rowe, M.C., Wolff, J.A., Boroughs, S.P., 2016. Megacrystic pyroxene basalts sample deep crustal gabbroic cumulates beneath the Mount Taynor volcanic field, New Mexico. *J. Volcanol. Geotherm. Res.* 316, 1–11.
- Shaw, C.S.J., 2009. Textural development of amphibole during breakdown reactions in a synthetic peridotite. *Lithos* 110, 215–228.
- Shaw, C.S.J., Eyzaguirre, J., 2000. Origin of megacrysts in the mafic alkaline lavas of the West Eifel Volcanic Field, Germany. *Lithos* 50, 75–95.
- Siebel, W., Schmitt, A.K., Danišik, M., Chen, F., Meier, S., Weiß, S., Eroğlu, S., 2009. Prolonged mantle residence of zircon xenocrysts from the western Eger rift. *Nat. Geosci.* 2, 886–890.
- Streck, M.J., 2008. Mineral textures and zoning as evidence for open system processes. *Rev. Mineral. Petrol.* 69, 595–622.
- Szumowska, M., Awdankiewicz, M., Christiansen, E., 2013. Geology and petrology of Cenozoic volcanic rocks of Ostrzyca Hill in the Kaczawa Foothills, SW Poland. XXth Meeting of the Petrology Group of the Mineralogical Society of Poland. *Mineralogia - Special Papers*. Niemcza, Poland, p. 88.
- Thöni, M., Miller, C., Blichert-Toft, J., Whitehouse, M.J., Konzett, J., Zanetti, A., 2008. Timing of high-pressure metamorphism and exhumation of the eclogite type-locality (Kupplerbrunn-Prickler Halt, Saualpe, south-eastern Austria): constraints from correlations of the Sm-Nd, Lu-Hf, U-Pb and Rb-Sr isotopic systems. *J. Metamor. Geol.* 26, 561–581.
- Ulrych, J., Balogh, K., 2000. Roztoky intrusive Centre in the České Středohoří Mts.: Differentiation, emplacement, distribution, orientation and age of dyke series. *Geol. Carpath.* 51, 383–397.
- Ulrych, J., Dostal, J., Adamovič, J., Jelínek, E., Špaček, P., Hegner, E., Balogh, K., 2011. Recurrent Cenozoic volcanic activity in the Bohemian Massif (Czech Republic). *Lithos* 123, 133–144.
- Upton, B.G.J., Hinton, R.W., Aspen, P., Finch, A., Valley, J.W., 1999. Megacrysts and associated xenoliths: evidence for migration of geochemically enriched melts in the upper mantle beneath Scotland. *J. Petrol.* 40, 935–956.
- Upton, B.G.J., Finch, A.A., Slaby, E., 2009. Megacrysts and salic xenoliths in Scottish alkali basalts: derivatives of deep crustal intrusions and small-melt fractions from the upper mantle. *Mineral. Mag.* 73, 943–956.
- Warren, J., 2016. Global variations in abyssal peridotite compositions. *Lithos* 248–251, 193–219.
- Wilson, M., Downes, H., 2006. Tertiary-Quaternary intra-plate magmatism in Europe and its relationship to mantle dynamics. "European Lithosphere Dynamics" Memoir. Geological Society, London, pp. 147–166.
- Wilson, M., Downes, H., Cebria, J.-M., 1995. Contrasting fractionation trends in coexisting continental alkaline magma series; Cantal, Massif Central, France. *J. Petrol.* 36, 1729–1753.
- Wimmenauer, W., 1974. The alkaline province of Central Europe and France. In: Sørensen, H. (Ed.), *The Alkaline Rocks*. Wiley, London, pp. 286–291.
- Woodland, A.B., Jugo, P.J., 2007. A complex magmatic system beneath Devés volcanic field, Massif Central, France: evidence from clinopyroxene megacrysts. *Contrib. Mineral. Petrol.* 153, 719–731.
- Woodland, A.B., Kornprobst, J., Tabit, A., 2006. Ferric iron in Orogenic Iherzolite Massifs and controls of oxygen fugacity in the upper mantle. *Lithos* 89, 222–241.
- Workman, R.K., Hart, S.R., 2005. Major and trace element composition of the depleted MORB mantle (DMM). *Earth Planet. Sci. Lett.* 231, 53–72.
- Wykes, J.L., O'Neil, H.St.C., Mavrogenes, J.A., 2015. The effect of FeO on the sulfur content at sulfide saturation (SCSS) and the selenium content at selenide saturation of silicate melt. *J. Petrol.* 7, 1407–1424.
- Zindler, A., Hart, S., 1986. Chemical geodynamics. *Annu. Rev. Earth Planet. Sci.* 14, 493–571.